This article is a *Plant Cell* Advance Online Publication. The date of its first appearance online is the official date of publication. The article has been edited and the authors have corrected proofs, but minor changes could be made before the final version is published. Posting this version online reduces the time to publication by several weeks.

Arabidopsis CALCIUM-DEPENDENT PROTEIN KINASE8 and CATALASE3 Function in Abscisic Acid-Mediated Signaling and H_2O_2 Homeostasis in Stomatal Guard Cells under Drought Stress[OPEN]

Jun-Jie Zou,[1,2] Xi-Dong Li,[1] Disna Ratnasekera,[1,3] Cun Wang,[1] Wen-Xin Liu, Lian-Fen Song, Wen-Zheng Zhang,[4] and Wei-Hua Wu[5]

State Key Laboratory of Plant Physiology and Biochemistry, College of Biological Sciences, National Plant Gene Research Centre (Beijing), China Agricultural University, Beijing 100193, China

ORCID IDs: 0000-0002-4824-400X (J.-J.Z.); 0000-0002-0077-4466 (X.-D.L.); 0000-0003-3176-6888 (D.R.); 0000-0003-0583-9510 (W.-X.L.); 0000-0001-5497-5768 (L.-F.S.); 0000-0002-0642-5523 (W.-H.W.)

Drought is a major threat to plant growth and crop productivity. Calcium-dependent protein kinases (CDPKs, CPKs) are believed to play important roles in plant responses to drought stress. Here, we report that *Arabidopsis thaliana* CPK8 functions in abscisic acid (ABA)- and Ca^{2+}-mediated plant responses to drought stress. The *cpk8* mutant was more sensitive to drought stress than wild-type plants, while the transgenic plants overexpressing *CPK8* showed enhanced tolerance to drought stress compared with wild-type plants. ABA-, H_2O_2-, and Ca^{2+}-induced stomatal closing were impaired in *cpk8* mutants. Arabidopsis CATALASE3 (CAT3) was identified as a CPK8-interacting protein, confirmed by yeast two-hybrid, coimmunoprecipitation, and bimolecular fluorescence complementation assays. CPK8 can phosphorylate CAT3 at Ser-261 and regulate its activity. Both *cpk8* and *cat3* plants showed lower catalase activity and higher accumulation of H_2O_2 compared with wild-type plants. The *cat3* mutant displayed a similar drought stress-sensitive phenotype as *cpk8* mutant. Moreover, ABA and Ca^{2+} inhibition of inward K^+ currents were diminished in guard cells of *cpk8* and *cat3* mutants. Together, these results demonstrated that *CPK8* functions in ABA-mediated stomatal regulation in responses to drought stress through regulation of CAT3 activity.

INTRODUCTION

In terrestrial plants, calcium plays a vital role as a second messenger in plant responses to various environmental stimuli (White and Broadley, 2003; Kudla et al., 2010). Calcium signals triggered by different stimuli are recognized by specific calcium sensors in living plant cells. There are three major families of calcium sensors in terrestrial plants, including calmodulins (CaMs) and CaM-like proteins (Zielinski, 1998; McCormack et al., 2005), calcineurin B-like (CBL) proteins (Kolukisaoglu et al., 2004; Luan, 2009; Weinl and Kudla, 2009), and calcium-dependent protein kinases (CDPKs or CPKs) (Harmon et al., 2000; Cheng et al., 2002; Harper and Harmon, 2005). CaMs and CBLs do not have enzymatic activities and so do not directly transmit the Ca^{2+} signals (Luan et al., 2002). By contrast, CDPKs, which harbor a CaM-like domain as well as a catalytic Ser/Thr kinase domain, can sense calcium signals and directly mediate a variety of cellular responses (Harmon et al., 2000; Cheng et al., 2002).

CDPKs are encoded by multigene families and found only in plants and some protists (Harmon et al., 2000; Cheng et al., 2002). The CDPKs exhibit different subcellular localizations, including cytosol, nucleus, the plasma membrane, endoplasmic reticulum, peroxisome, mitochondrial outer membrane, and oil bodies (Harper et al., 2004), likely reflecting diverse functions. CDPKs are believed to be important regulators in multiple plant signal transduction pathways downstream of cytosolic Ca^{2+} ($[Ca^{2+}]_{cyt}$) elevations (Harmon et al., 2000; Cheng et al., 2002; Ludwig et al., 2004; Boudsocq and Sheen, 2013; Romeis and Herde, 2014).

The *Arabidopsis thaliana* genome encodes 34 CDPKs, and a number of studies have shown that CDPKs are involved in plant development and in responses to biotic and abiotic stresses. Arabidopsis CDPKs can act as positive or negative regulators in response to abiotic stress and abscisic acid (ABA) signaling. Arabidopsis CPK32 has been characterized as an ABA signaling component that regulates ABA-responsive gene expression via ABF4 (Choi et al., 2005). Arabidopsis CPK3 and CPK6 function as positive transducers in plant ion channel regulation and stomatal ABA signaling (Mori et al., 2006), as well as salt and/or drought stress(es) (Mehlmer et al., 2010; Xu et al.,

[1] These authors contributed equally to this work.
[2] Current address: Key Laboratory of Plant Molecular Physiology, Institute of Botany, Chinese Academy of Sciences, Beijing 100093, China.
[3] Current address: Department of Agricultural Biology, Faculty of Agriculture, University of Ruhuna, Matara 81100, Sri Lanka.
[4] Current address: The Samuel Roberts Noble Foundation, 2510 Sam Noble Parkway, Ardmore, OK 73401.
[5] Address correspondence to whwu@cau.edu.cn.
The author responsible for distribution of materials integral to the findings presented in this article in accordance with the policy described in the Instructions for Authors (www.plantcell.org) is: Wei-Hua Wu (whwu@cau.edu.cn).
[OPEN]Articles can be viewed online without a subscription.
www.plantcell.org/cgi/doi/10.1105/tpc.15.00144

2010). Arabidopsis CPK4 and CPK11 have been identified as important positive regulators in CDPK/calcium-mediated ABA signaling (Zhu et al., 2007). By contrast, Arabidopsis CPK21 functions as a negative regulator in abiotic stress signal transduction (Franz et al., 2011). Furthermore, CPK12 serves as a negative ABA-signaling regulator in seed germination and postgermination growth, which is different from the function of its homologs, CPK4 and CPK11 (Zhao et al., 2011). In addition to abiotic stress, some Arabidopsis CDPKs have been reported to be involved in the plant innate immune response (CPKs 4, 5, 6, and 11 [Boudsocq et al., 2010], CPK1 [Coca and San Segundo, 2010], and CPK5 [Dubiella et al., 2013]), herbivory-induced signaling network (CPK3 and CPK13; Kanchiswamy et al., 2010), regulation of pollen tube growth (CPK17 and CPK34 [Myers et al., 2009], CPK11 and CPK24 [Zhao et al., 2013], CPK2 and CPK20 [Gutermuth et al., 2013], and CPK32 [Zhou et al., 2014]), and stem elongation and vascular development (CPK28; Matschi et al., 2013).

We previously demonstrated that Arabidopsis CPK10 functions in ABA- and Ca^{2+}-mediated stomatal regulation in response to drought stress (Zou et al., 2010). Here, we report that CPK8 (At5g19450) as well as its interacting protein CATALASE3 (CAT3; At1g20620) play important roles in ABA- and H_2O_2-mediated signal transduction and in maintaining H_2O_2 homeostasis in response to drought stress.

RESULTS

CPK8 Acts as a Positive Regulator in Response to Drought Stress and Involving in ABA- and H_2O_2-Mediated Stomatal Movement

After a 20-d period of drought stress, the *CPK8* T-DNA insertion mutant plants (*cpk8*, SALK_036581; Supplemental Figure 1A) showed more sensitive phenotype compared with wild-type plants (Figure 1A), while there was no obvious morphological difference observed between *cpk8* mutant and wild-type plants under normal growth condition (Figure 1A). When 3-week-old plants grown under normal conditions were subjected to drought stress for about 1 week, the leaf temperature of *cpk8* mutant plants was lower than that in the wild-type plants (Figure 1B), suggesting that water loss of the *cpk8* plants may be faster than that of the wild-type plants. β-Glucuronidase (GUS) staining of $CPK8_{pro}$*:GUS* transgenic plants showed that the *CPK8* promoter drove expression in leaves and roots (Figure 1C) and particularly in stomatal guard cells (Figure 1D), suggesting a potential role of CPK8 in regulation of stomatal movement. The results of reverse transcriptase quantitative PCR (RT-qPCR) showed that *CPK8* transcript accumulation was induced by drought (Supplemental Figure 1B), ABA (Supplemental Figure 1C), and H_2O_2 (Supplemental Figure 1D) treatments.

To further test whether the drought sensitivity of *cpk8* plants resulted from *CPK8* disruption, *CPK8* overexpression lines (ecotype Columbia [Col] + *CPK8*; 8OE) and complementation lines (*cpk8* + *CPK8;* 8COM) were generated. The RT-qPCR results showed that transcription of *CPK8* was disrupted in the *cpk8* homozygous plants (Figure 1E). When subjected to drought stress for 20 d, the *cpk8* mutant plants were more sensitive to drought stress, whereas the *CPK8* overexpression lines (8OE1 and 8OE2) showed enhanced tolerance to drought stress compared with wild-type plants (Figure 1F). The overexpression lines (8OE1 and 8OE2) grew well and the rosette leaves remained green even after 22 d without watering (Figure 1F). The *cpk8* complementation lines (8COM1 and 8COM2) showed a similar phenotype as wild-type plants after the drought stress treatment (Figure 1F). These results indicate that disruption of *CPK8* expression increases plant sensitivity to drought stress and that increased *CPK8* expression enhances plant tolerance to drought stress.

The stomatal pores control most of the water loss via transpiration to the atmosphere (Schroeder et al., 2001). To test the hypothesis that CPK8 may be involved in regulation of stomatal movements under drought stress, water loss assays of detached leaves were conducted. As shown in Figure 1G, water loss of the detached rosette leaves of *cpk8* plants was much faster than that of wild-type leaves, while water loss of the *CPK8* overexpression (8OE1) leaves was slower than that of wild-type leaves under dehydration conditions.

H_2O_2 is one of the major reactive oxygen species (ROS) and serves as an important messenger in ABA-regulated stomatal movement (Pei et al., 2000; Murata et al., 2001; Zhang et al., 2001a; Kwak et al., 2003; Miao et al., 2006). Accumulation of H_2O_2 in stomatal guard cell can cause $[Ca^{2+}]_{cyt}$ elevations and result in stomatal closure (Pei et al., 2000; Murata et al., 2001; Kwak et al., 2003). We further hypothesized that CPK8 may serve as a calcium sensor and function in ABA- and H_2O_2-mediated regulation of stomatal movement. To test this hypothesis, stomatal aperture assays were conducted to examine stomatal responses of different lines to ABA, H_2O_2, and Ca^{2+}. As shown in Figures 1H to 1J, stomatal closure induced by ABA (Figure 1H), H_2O_2 (Figure 1I), or Ca^{2+} (Figure 1J) was impaired in the *cpk8* mutant plants. These results suggest that CPK8 may serve as an important signaling component to mediate ABA as well as H_2O_2 and Ca^{2+} signals in regulation of stomatal movement.

Identification of CAT3 as a CPK8-Interacting Protein

We next undertook identification of CPK8-interacting protein(s) to gain insight into CPK8 might function in ABA and H_2O_2 signaling. In previous studies, a number of experimental approaches had been employed to identify CDPK-interacting proteins (Patharkar and Cushman, 2000; Lee et al., 2003; Shao and Harmon, 2003; Rodriguez Milla et al., 2006; Böhmer and Romeis, 2007; Vlad et al., 2008; Uno et al., 2009). Among these different approaches, yeast two-hybrid screening with baits containing only the kinase domain of the protein had been demonstrated to be successful for identification of CDPK substrates, such as for ice plant (*Mesembryanthemum crystallinum*) CPK1 (Patharkar and Cushman, 2000) and tobacco (*Nicotiana tabacum*) CDPK1 (Lee et al., 2003). Here, using the kinase domain of CPK8 as bait, a catalase protein encoded by At1g20620 (*CAT3*) was identified as a potential CPK8-interacting protein (Figure 2A). There are three catalase genes in the Arabidopsis genome, including *CAT1* (At1g20630), *CAT2* (At4g35090), and

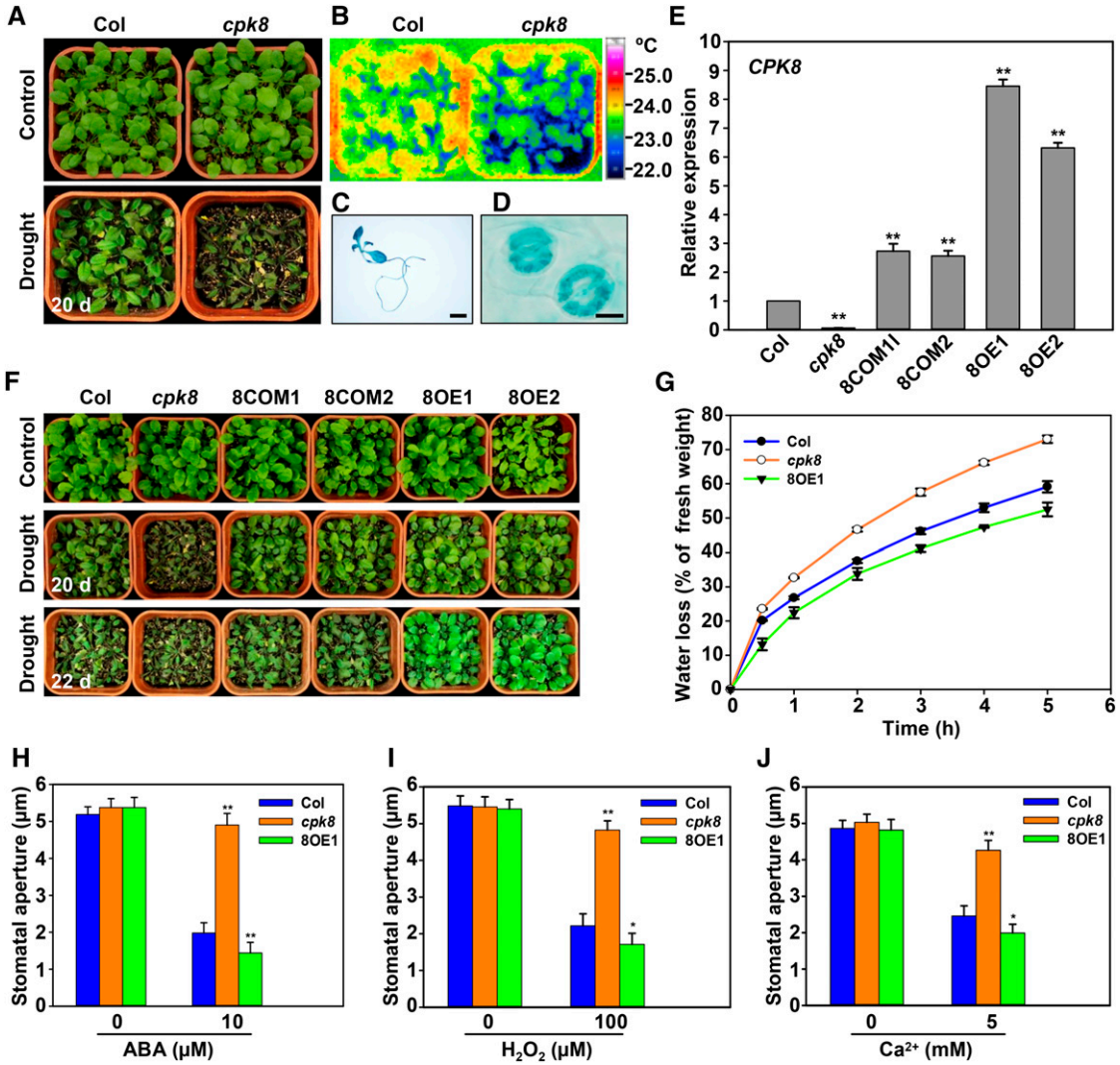

Figure 1. Arabidopsis CPK8 Acts as a Positive Regulator in ABA- and H_2O_2-Mediated Stomatal Movement in Response to Drought Stress.

(A) Drought phenotype of Arabidopsis *cpk8* (SALK_036581) compared with wild-type plants under normal and drought conditions in soil. For the drought stress treatment, the photographs were taken after withholding water for 20 d. The experiments were repeated three times with similar results.
(B) False-color infrared image of the wild-type and *cpk8* plants. The leaf temperature of *cpk8* was lower than that of wild-type plants.
(C) and **(D)** Expression patterns of *CPK8* as determined by $CPK8_{pro}$*:GUS* transgenic plants. Transgenic plants were stained with 5-bromo-4-chloro-3-indolyl-β-D-glucuronic acid solution for 12 h. Bars = 2 mm in **(C)** and 10 μm in **(D)**.
(E) RT-qPCR analysis of *CPK8* expression in Arabidopsis *cpk8* mutant (*cpk8*), complementation lines, and overexpression lines. The *18S rRNA* was used as an internal control. The experiments were repeated three times. Each data point represents mean ± SE (n = 3). Asterisk indicates significant difference relative to Col (Student's t test, **P < 0.01).
(F) Drought stress sensitivity of the wild type, *cpk8*, 8COM1, and 8OE1 in soil after water was withheld for 20 d (normal drought stress) or 22 d (severe drought stress). The experiments were repeated three times with similar results.
(G) Time courses of water loss from detached leaves of wild-type, *cpk8*, and 8OE1 plants. Water loss is expressed as the percentage of initial fresh weight. The experiments were repeated three times with similar results. Each data point represents mean ± SE (n = 3).
(H) to **(J)** ABA-, H_2O_2-, and Ca^{2+}-induced stomatal closing in wild-type, *cpk8*, and 8OE1 plants. The experiments were repeated three times. Each data point represents mean ± SE (n = 50). Asterisk indicates significant difference relative to Col (Student's t test, *P < 0.05 and **P < 0.01).

CAT3 (Frugoli et al., 1996). To verify the specificity of the CPK8 interaction with CAT3, three catalase isoforms were used as prey for yeast two-hybrid assays. As shown in Figure 2A, when the CPK8 bait was cotransformed with the CAT1, CAT2, and CAT3 preys individually, only the AH109 yeast cells carrying pGBKT7-CPK8 and pGADT7-CAT3 grew well on the selection medium (SC/-Leu/-Trp/-His/-Ade) and exhibited β-galactosidase (β-gal) activity.

The interaction between CPK8 and CAT3 in planta was confirmed using coimmunoprecipitation (co-IP) assays. Proteins

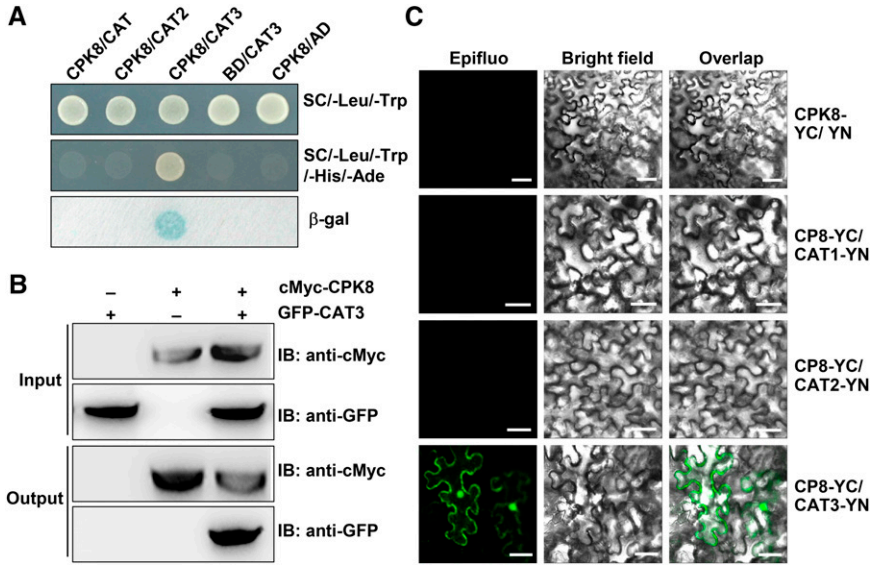

Figure 2. Protein Interaction between CPK8 and CAT3.

(A) Yeast two-hybrid assay of CPK8 interaction with CAT1, CAT2, and CAT3. The kinase domain of CPK8 was used as bait. CPK8/pGADT7 was used as negative control. Transformants were plated on selection medium and grown for 4 d before β-gal staining.

(B) Co-IP assay showing the interaction between CPK8 and CAT3 expressed in Arabidopsis mesophyll protoplasts. Extracted proteins were incubated with anti-cMyc agarose beads. The immunoprecipitates were analyzed by immunoblotting (IB) with anti-GFP or anti-cMyc antibodies.

(C) BiFC assay of CPK8 interaction with CAT1, CAT2, and CAT3 in *N. benthamiana* leaves in planta. The C-terminal half of GFP was fused to CPK8 (CPK8-YC), and the N-terminal half of GFP was fused to CAT1, CAT2, and CAT3. The expression of CPK8-YC/YN was used as control. Bar = 50 μm.

were extracted from Arabidopsis mesophyll protoplasts harboring *35S$_{pro}$:cMyc-CPK8* and *35S$_{pro}$:CAT3-GFP* constructs and used for co-IP assays. As shown in Figure 2B, immunoprecipitation of CPK8 with anti-cMyc agarose conjugate yielded a co-IP band corresponding to the tagged CAT3 that was labeled with the anti-GFP antibody.

Before we performed bimolecular fluorescence complementation (BiFC) assays (Waadt and Kudla, 2008) to further confirm the interaction between CPK8 and CAT3 in planta, we rechecked the subcellular localizations of CPK8 and CAT3. CPK8 was localized to the plasma membrane as described previously (Dammann et al., 2003) and CAT3 was localized to the peroxisome, cytoplasm, and the plasma membrane (Supplemental Figure 2). The BiFC assays showed that CPK8 could specifically interact with CAT3, and the CPK8/CAT3 complex was localized to the plasma membrane of the cotransformed *Nicotiana benthamiana* epidermal cells (Figure 2C). In addition, firefly luciferase complementation imaging assays confirmed that CPK8 specifically interacted with CAT3, but not with CAT1 and CAT2 (Supplemental Figure 3).

CPK8 Can Phosphorylate CAT3 at Ser-261 and Regulate Its Activity

Both in vitro and in planta protein phosphorylation assays were conducted to demonstrate CAT3 phosphorylation by CPK8. Strep-tagged CPK8 (Strep-CPK8) was transiently expressed in *N. benthamiana* and purified (Supplemental Figure 4A), and GST-CAT1, GST-CAT2, and GST-CAT3 proteins were expressed in *Escherichia coli* and purified (Supplemental Figure 4B). As shown in Figure 3A, CPK8 had autophosphorylation activity and could phosphorylate CAT3 but not CAT1 and CAT2.

Reiland et al. (2009) reported that CAT3 is a phosphoprotein and the phosphorylated amino acid is detected at Thr-408. When Thr-408 was mutated to Ala (CAT3^{T408A}), the mutant protein was still phosphorylated by CPK8 (Figure 3A), indicating that CPK8 may phosphorylate one or more other residue(s). To determinate CPK8 phosphorylation site(s) in CAT3, additional CAT3 truncated proteins were generated (Figure 3B; Supplemental Figure 4C). CAT3-N (from Met-1 to Ala-260) and CAT3-C2 (from Glu-320 to Ile-492) were not phosphorylated by CPK8, while the CAT3-C-terminal truncated proteins containing region from Ser-261 to Thr-319 could be phosphorylated by CPK8, indicating that CPK8 phosphorylation of CAT3 occurs in this region (Figure 3C; Supplemental Figures 4C and 4D). In CAT3, there are five potential phosphorylation sites in the region from Ser-261 to Thr-319 (Figure 3D; Supplemental Figure 4E). When Ser-261 in CAT3 was mutated to Ala (CAT3^{S261A}-C1), the mutant protein was not phosphorylated by CPK8 (Figure 3E; Supplemental Figure 4F). When Thr-273, Thr-290, Thr-311, or Thr-319 was mutated to Ala (CAT3^{T273A}-C1, CAT3^{T290A}-C1, CAT3^{T311A}-C1, and CAT3^{T319A}-C1), these mutant proteins could still be phosphorylated by CPK8 (Figure 3E; Supplemental Figure 4F). In addition, the quadruple mutant CAT3^{T273A,T290A,T311A,T319A}-C1 was also phosphorylated by CPK8 (Figure 3E). These results indicate that Ser-261 in CAT3 is the only residue phosphorylated by CPK8 in vitro. It should be noted that Ser-261 is not conserved in Arabidopsis CATs, and Ser-261 in CAT3 is substituted with Ala-261 in CAT1 and CAT2 (Frugoli et al., 1996).

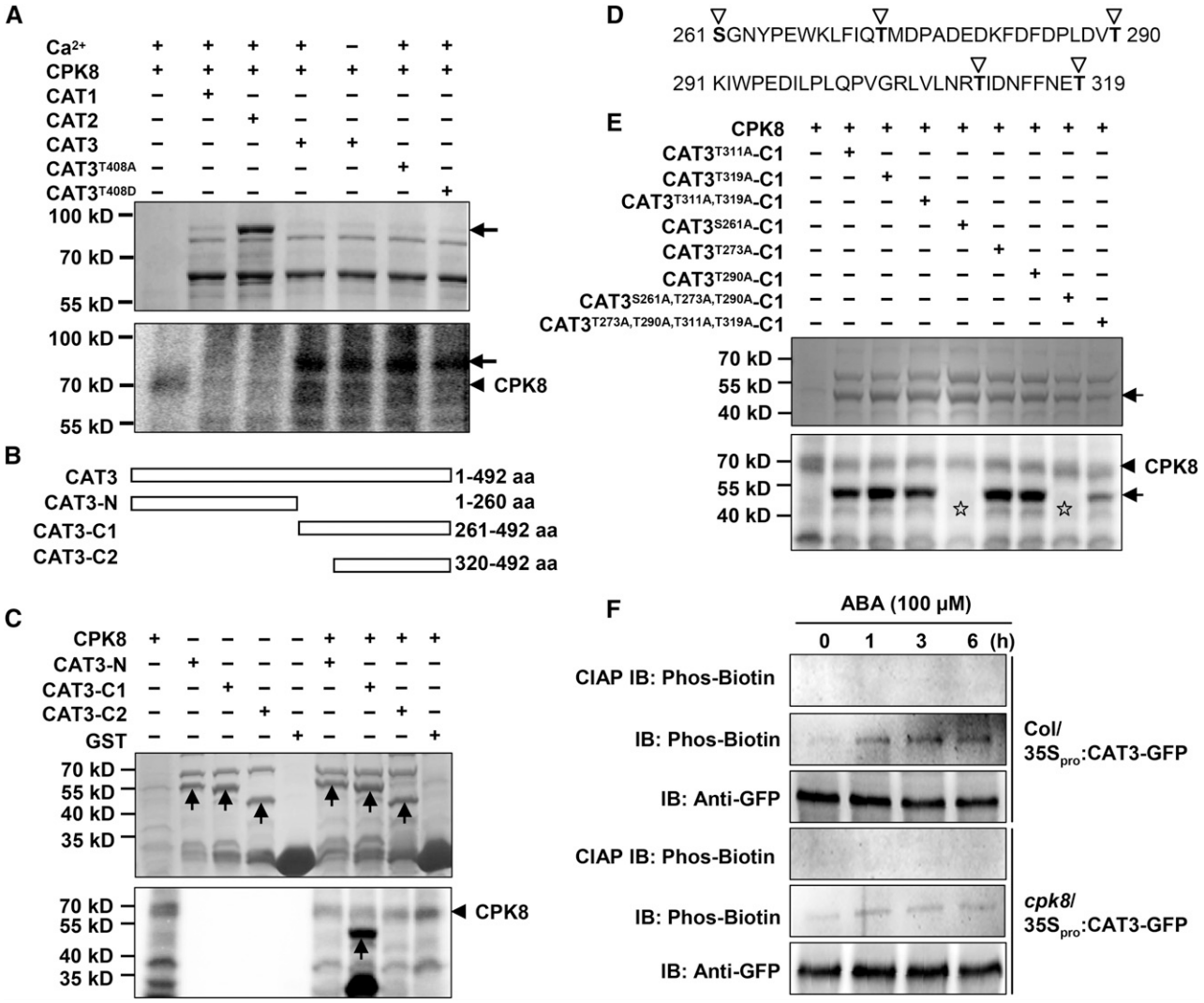

Figure 3. CPK8 Phosphorylates CAT3 in Vitro and in Planta.

(A) CPK8 can phosphorylate CAT3 in vitro. Coomassie blue-stained recombinant proteins of CAT1, CAT2, and CAT3 proteins are indicated by the arrow in the top panel. In the bottom panel, the arrowhead shows the autophosphorylated CPK8, and the arrow shows the phosphorylated CAT3 variants.
(B) Model of CAT3 N-terminal and C-terminal deletions.
(C) Phosphorylation of CAT3 N-terminal and C-terminal deletions by CPK8 in vitro. Coomassie blue-stained recombinant proteins of CAT3 are indicated with arrows in the top panel. In the bottom panel, the arrowhead indicates the autophosphorylated CPK8, and the arrow denotes the phosphorylated CAT3-C1 terminus.
(D) Potential phosphorylation sites (indicated with triangles) in CAT3-C1 residues from Ser-261 to Thr-319.
(E) Phosphorylation of CAT3 at Ser-261 by CPK8. Coomassie blue-stained CAT3-C1 variants are indicated by the arrow in the top panel. In the bottom panel, the arrowhead indicates the autophosphorylated CPK8, and the arrow indicates the phosphorylated CAT3-C1 variants. $CAT3^{S261A}$-C1, CAT3-C1 with Ser-261 mutated to Ala. $CAT3^{T273A}$-C1, CAT3-C1 with Thr-273 mutated to Ala. $CAT3^{T290A}$-C1, CAT3-C1 with Thr-290 mutated to Ala. $CAT3^{T311A}$-C1, CAT3-C1 with Thr-311 mutated to Ala. $CAT3^{T319A}$-C1, CAT3-C1 with Thr-319 mutated to Ala. $CAT3^{T311A,T319A}$-C1, CAT3-C1 with Thr-311 and Thr-319 mutated to Ala. $CAT3^{S261A,T273A,T290A}$-C1, CAT3-C1 with Ser-261, Thr-273, and Thr-290 mutated to Ala. $CAT3^{T273A,T290A,T311A,T319A}$-C1, CAT3-C1 with Thr-273, Thr-290, Thr-311, and Thr-319 mutated to Ala.
(F) CPK8 can phosphorylate CAT3 in planta. Wild-type plants (Col) or *cpk8* plants expressing *$35S_{pro}$:CAT3-GFP* were treated with 100 μM ABA for 1, 3, and 6 h. Total proteins were extracted and CAT3-GFP proteins were immunoprecipitated using anti-GFP mAb agarose. The phosphorylated CAT3 proteins were detected by immunoblotting (IB) using biotinylated Phos-tag. Calf intestinal alkaline phosphatase (CIAP)-treated proteins were used as control.

To determine whether CAT3 is phosphorylated by CPK8 in planta, transgenic lines (Col/*35S$_{pro}$:CAT3-GFP* and *cpk8/35S$_{pro}$:CAT3-GFP*) were generated. The CAT3 phosphorylation level was detected using Phos-Biotin technology as described previously (Kinoshita-Kikuta et al., 2007). Under normal conditions, CAT3 phosphorylation was very low in Col/*35S$_{pro}$:CAT3-GFP* and *cpk8/35S$_{pro}$:CAT3-GFP* plants (Figure 3F). After ABA treatment, CAT3 phosphorylation was obviously enhanced in Col/*35S$_{pro}$:CAT3-GFP* (Figure 3F). However, this ABA-induced CAT3 phosphorylation was weakened in *cpk8/35S$_{pro}$:CAT3-GFP*, indicating that ABA-induced CAT3 phosphorylation is CPK8 dependent (Figure 3F).

To study the significance of phosphorylation of CAT3, catalytic activity of the recombinant CAT3 was analyzed in the presence of CPK8. As shown in Figure 4A, CPK8 had no effect on the CAT1 or CAT2 catalase activity, whereas CPK8 significantly enhanced CAT3 activity in the presence of ATP. However, mutation of Thr-408 (CAT3^{T408A} or CAT3^{T408D}) did not affect CPK8-activated CAT3 activity (Figure 4A). When Ser-261 was mutated to Ala (CAT3^{S261A}), CPK8 did not stimulate catalase activity of CAT3^{S261A} (Figure 4B), and when Ser-261 was mutated to Asp (CAT3^{S261D}), the mutated CAT3^{S261D} showed high catalase activity even in the absence of CPK8 (Figure 4B). These results clearly demonstrate that Ser-261 in CAT3 is an essential residue for CAT3 activation by CPK8.

The *cpk8* and *cat3* Mutants Have Low Catalase Activity and High H_2O_2 Production

To further investigate the effect of CPK8 on catalase activity in planta, *CPK8*- and *CAT3*-related materials were used for catalase activity assays. The site of T-DNA insertion in *cat3* (SALK_092911) was located in the first intron of *CAT3* genomic DNA (Supplemental Figure 5A). RT-PCR analysis showed that the expression of *CAT3* was completely disrupted in *cat3* mutant (Supplemental Figure 5B). Transcript levels of *CAT3* in Col, *cat3*, and *CAT3* overexpression lines are presented in Figure 5A. The *cat3* mutant plants had a decrease in catalase activity of ~20% compared with wild-type plants, consistent with a previous report (Figure 5B; Mhamdi et al., 2010). Similar to the *cat3* mutant, the *cpk8* mutant also had decreased catalase activity (Figure 5B). When *CPK8* was overexpressed in the *cat3* mutant background, the catalase activity in the 8OE/*cat3* line was similar as that in the *cat3* mutant. Consistent with the decreased catalase activities in the *cpk8*, *cat3*, and *8OE/cat3* plants, these plants also show greater ROS accumulation compared with wild-type plants (Figure 5C). When treated with ABA, *cpk8*, *cat3*, and *8OE/cat3* plants accumulated more ROS compared with the ABA-treated wild-type plants (Figure 5C).

The 3,3′-diaminobenzidine (DAB) uptake method (Thordal-Christensen et al., 1997; Guan and Scandalios, 2000) was used to examine the production of H_2O_2 in leaves after treatment with ABA. As shown in Figure 5D, after ABA treatment, the *cpk8* and *cat3* mutants as well as *8OE/cat3* plants accumulated more, and *CPK8* and *CAT3* overexpression lines accumulated less H_2O_2 in the leaves compared with wild-type plants.

The ROS production in stomatal guard cells of *cpk8*, *cat3*, and wild-type plants was further analyzed using the dye 2',7'-dichlorofluorescein diacetate (H_2DCF-DA) (Miao et al., 2006). After treatment with ABA for 5 min, the pixel intensity of fluorescence emission in guard cells of *cpk8* and *cat3* mutants was higher than that of wild-type plants (Figures 5E and 5F). All of these results suggest that CPK8 can regulate H_2O_2 homeostasis by modulating CAT3 activity.

The *cat3* Mutant Shows a Similar Phenotype as the *cpk8* Mutant in Response to Drought Stress

Previous reports revealed that *CAT3* was expressed in leaves and guard cells (Zimmermann et al., 2006; Du et al., 2008;

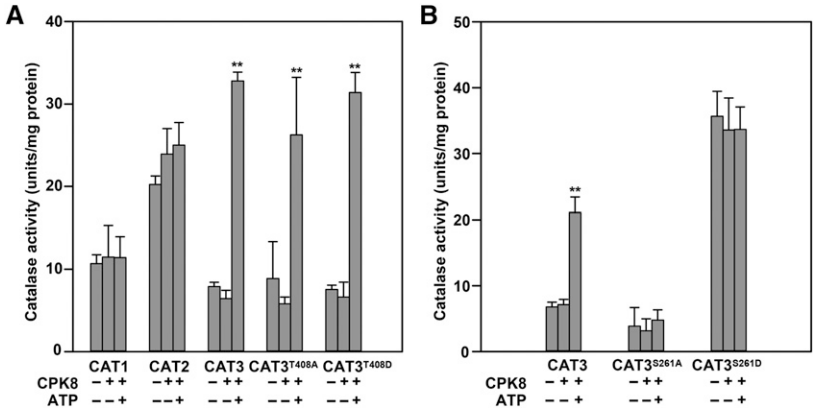

Figure 4. CPK8 Positively Regulates CAT3 Catalase Activity.

(A) Recombinant CAT1, CAT2, and CAT3 proteins expressed in *E. coli* were purified, and the catalase activities were measured with or without CPK8 in the presence or absence of ATP. Each data point represents the mean ± SE (n = 6). Asterisk indicates significant difference relative to CAT activity in the absence of CPK8 and ATP (Student's t test, **P < 0.01).

(B) Phosphorylation of CAT3 at Ser-261 is essential for CAT3 activity. CAT3^{S261A}, recombinant CAT3 with Ser-261 mutated to Ala. Each data point represents the mean ± SE (n = 6). Asterisk indicates significant difference relative to CAT activity in the absence of CPK8 and ATP (Student's t test, **P < 0.01).

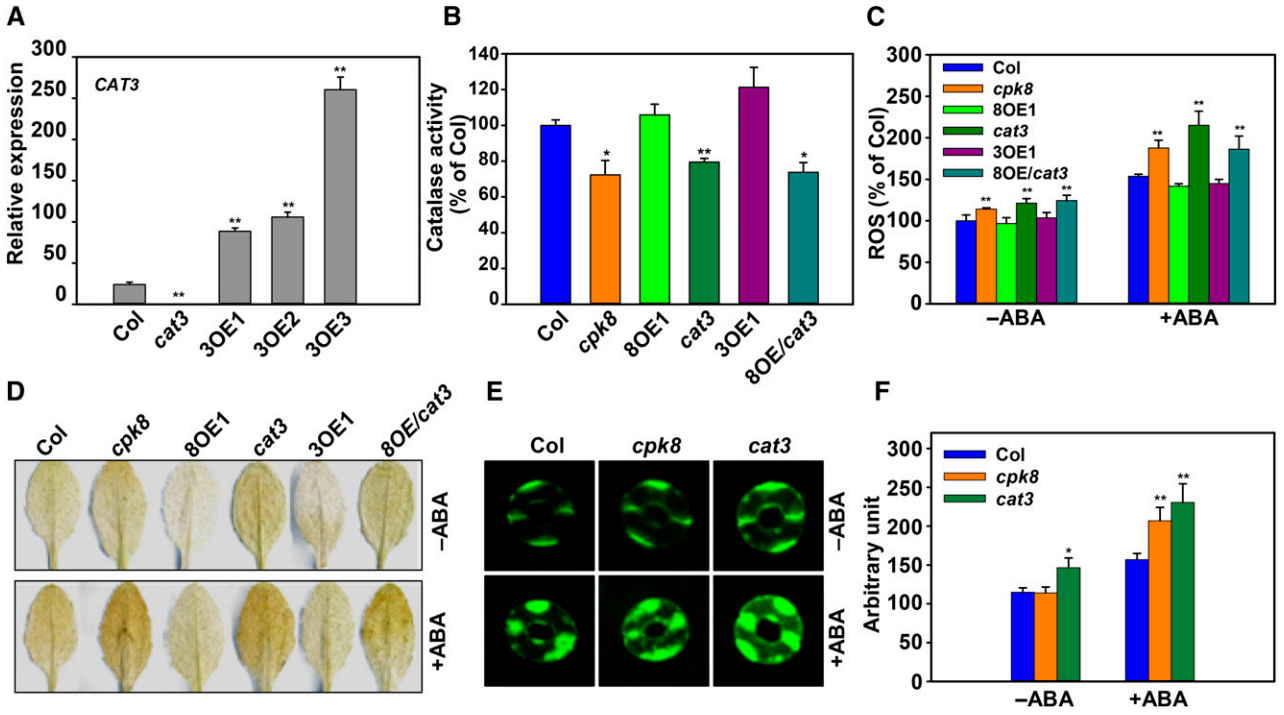

Figure 5. Comparison of Catalase Activity and H_2O_2 Accumulation in *CPK8* and *CAT3*-Related Plant Materials.

(A) RT-qPCR analysis of *CAT3* transcription in wild-type plants, *cat3*, and *CAT3* overexpression lines. The experiments were repeated three times with similar results. Each data point represents mean ± SE (n = 3). Asterisk indicates significant difference relative to Col (Student's t test, **P < 0.01).
(B) Catalase activity in wild-type, *cpk8*, 8OE1, *cat3*, 3OE1, and 8OE/*cat3* plants. Each data point represents mean ± SE (n = 3).
(C) ABA-induced H_2O_2 production in wild-type, *cpk8*, 8OE1, *cat3*, 3OE1, and 8OE/*cat3* plants.
(D) ABA-induced H_2O_2 production in leaves of wild-type plants and *cpk8* and *cat3* mutants assayed with DAB. The experiments were repeated three times with similar results.
(E) Exogenous ABA-induced production of ROS in stomatal guard cells. Abaxial epidermal peels from wild-type and mutant plants were loaded with H_2DCF-DA before and 5 min after the addition of 10 μM ABA. The photographs show representative fluorescence from stomatal guard cells of the wild type and mutants. The experiments were repeated three times with similar results.
(F) Effects of ABA on the DCF fluorescence in guard cells of the wild type, *cpk8*, and *cat3*. The data points represent mean ± SE from measurements of pixel intensity in whole cells determined before and 5 min after ABA (10 μM) treatment (n = 3). Asterisk indicates significant difference relative to Col (Student's t test, *P < 0.05 and **P < 0.01).

Jannat et al., 2011), and the transcription of *CAT3* was induced by ABA and drought (Xing et al., 2007), suggesting that CAT3 may function in ABA-mediated plant responses to drought stress. The transcript level of *CAT3* was induced by ABA (Supplemental Figure 5C) and H_2O_2 (Supplemental Figure 5D), consistent with the previous study (Xing et al., 2007). It was further hypothesized that CAT3, as a substrate of CPK8, may act downstream of CPK8 in ABA-mediated signal transduction in stomatal guard cells under drought stress. The *cat3* mutant plants and *CAT3* overexpression lines were tested for their sensitivity to drought stress. After a 20-d period of drought stress treatment (the normal drought stress treatment in this study), the *cat3* mutant showed similar sensitivity to drought stress as the *cpk8* mutant (Figure 6A). In addition, the *cpk8 cat3* double mutants showed similar sensitivity to drought stress as *cpk8* and *cat3* single mutant plants (Figure 6A). When *CPK8* was overexpressed in *cat3* (8OE/*cat3*) or *CAT3* overexpressed in *cpk8* (3OE/*cpk8*), both transgenic lines were as sensitive to drought stress as *cat3* and *cpk8* plants (Supplemental Figure 6), which not only further demonstrates that CPK8 acts as an upstream regulator of CAT3 but also demonstrates that activation of CAT3 requires its phosphorylation by CPK8. As shown in Figure 6B, wild-type plants did not survive a 22-d period of drought stress treatment (the "severe" drought stress treatment) even after rewatering. However, the *CAT3* overexpression lines not only survived, but also recovered well after rewatering. Consistent with these results, water loss assays showed that the detached leaves of *cat3*, similar to the *cpk8*, lost water faster than wild-type plants under dehydration treatment, whereas the 3OE1 leaves lost water slower than wild-type plants (Figure 6C). Furthermore, the *cat3* mutant showed impaired stomatal closing induced by ABA (Figure 6D), H_2O_2 (Figure 6E), and Ca^{2+} (Figure 6F) as well as impaired ABA inhibition of stomatal opening (Supplemental Figure 7), which was similar to the observation in the *cpk8* mutant. These results suggest that CPK8 and CAT3 function in the same signaling pathway in plant responses to drought stress.

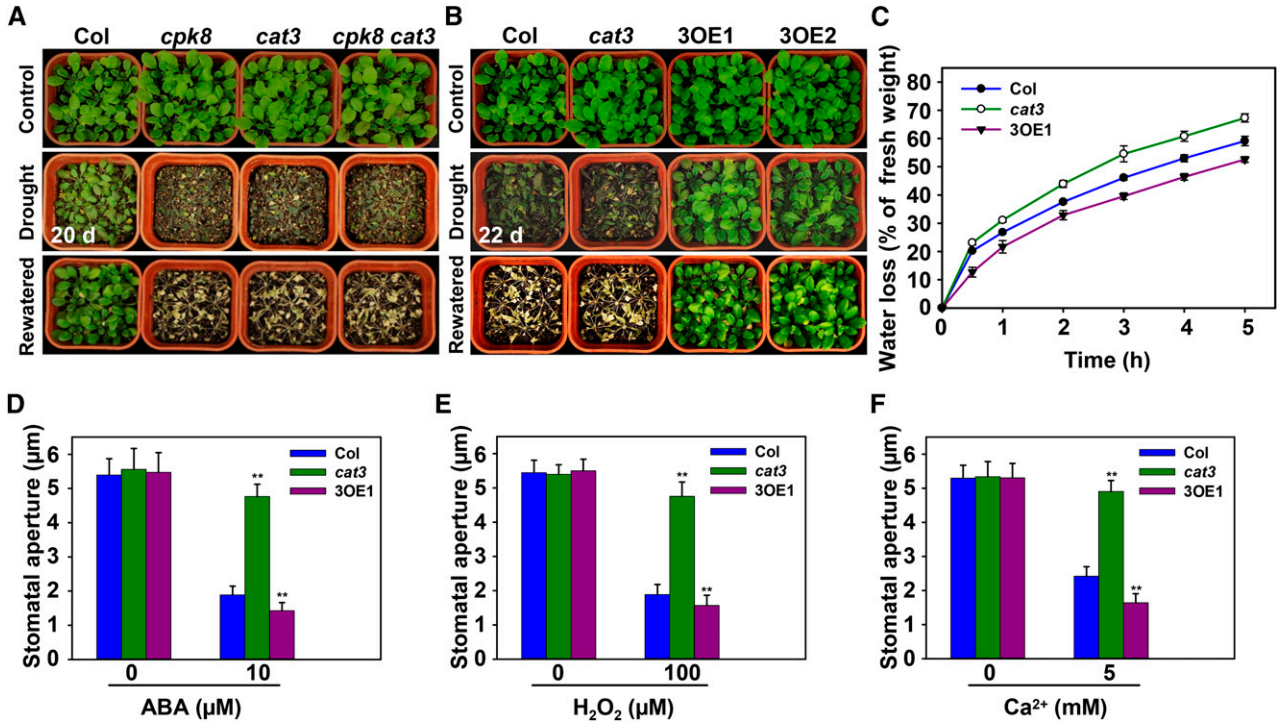

Figure 6. The *cat3* Mutant Shows a Similar Phenotype to the *cpk8* Mutant in Response to Drought Stress and Stomatal Movement.

(A) Phenotype comparison of wild-type, *cpk8*, *cat3*, and *cpk8 cat3* plants placed under drought stress for 20 d and then rewatered for 3 d. The experiments were repeated three times with similar results.

(B) Phenotype comparison of wild-type, *cat3*, and 3OE1 plants under drought stress for 22 d and then rewatered for 3 d. The experiments were repeated three times with similar results.

(C) Time courses of water loss from detached leaves of wild-type, *cat3*, and 3OE1 plants. The experiments were repeated three times with similar results. Each data point represents mean ± SE (n = 3).

(D) to **(F)** ABA-, H_2O_2-, and Ca^{2+}-induced stomatal closing in *cat3* mutant. The experiments were repeated three times. Each data point represents mean ± SE (n = 50). Asterisk indicates significant difference relative to Col (Student's t test, *P < 0.05 and **P < 0.01).

CPK8 and CAT3 Modulate ABA and Ca^{2+} Inhibition of the Inward K^+ Currents in Stomatal Guard Cells

ABA inhibition of the inward K^+ currents in stomatal guard cells has been well documented (Blatt, 1990; Schwartz et al., 1994; Zhang et al., 2001b). Elevation of $[Ca^{2+}]_{cyt}$ in guard cells inhibits the inward K^+ currents (Schroeder and Hagiwara, 1989; Kelly et al., 1995; Grabov and Blatt, 1997, 1999; Ivashikina et al., 2005). Some studies have demonstrated that CDPKs function in the regulation of ion channel activities in stomatal guard cells (Pei et al., 1996; Li et al., 1998; Mori et al., 2006; Zou et al., 2010; Geiger et al., 2010, 2011; Brandt et al., 2012; Scherzer et al., 2012). We found that ABA- and Ca^{2+}-induced stomatal closing and ABA-inhibited stomatal opening was impaired in the *cpk8* and *cat3* mutants (Figures 1H to 1J and 6E to 6G; Supplemental Figure 7). Using patch-clamp whole-cell recording techniques, we tested the effects of CPK8 and CAT3 on ABA- and Ca^{2+}-mediated regulation of the inward K^+ channels in guard cells. Inhibition of the inward K^+ currents by ABA (Figures 7A and 7B) and Ca^{2+} (Figures 7C and 7D) was observed in wild-type plants. However, inhibition of the inward K^+ currents by ABA (Figures 7A and 7B) and Ca^{2+} (Figures 7C and 7D) was impaired in the *cpk8* and *cat3* mutants. These results suggest that CPK8 and CAT3 may function downstream of ABA and Ca^{2+} in regulation of inward K^+ channel activities in stomatal guard cells.

DISCUSSION

CDPKs have been predicted to function in response to $[Ca^{2+}]_{cyt}$ elevations in many physiological processes in plants (Cheng et al., 2002; Boudsocq and Sheen, 2013; Romeis and Herde, 2014). Considering their diverse expression profiles as well as subcellular localizations together with their different responses to various environmental stimuli, each CDPK may have a specific function (Boudsocq and Sheen, 2013). Arabidopsis CPK7 shares 90% protein sequence identity with CPK8 (Cheng et al., 2002); however, the expression pattern of *CPK7* is different from that of *CPK8*. Expression driven by the *CPK8* promoter was abundant in stomatal guard cells (Figure 1D), whereas GUS activity driven by the *CPK7* promoter was not evident in stomatal guard cells (Supplemental Figure 8). Li et al. (2014) showed that CPK7 functions in root water transport, revealing different roles for CPK7 and CPK8 in spite of their high protein

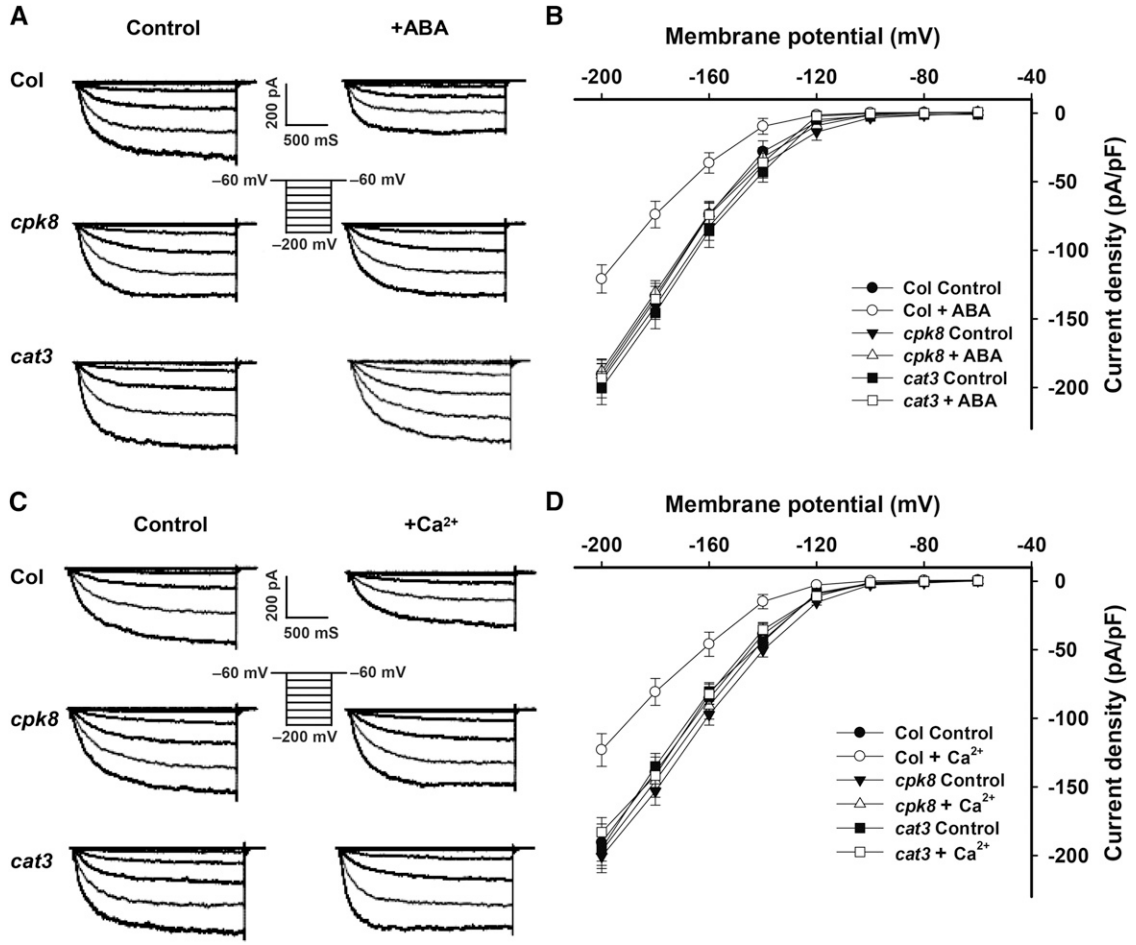

Figure 7. Inhibition of the Inward K^+ Currents in Stomatal Guard Cells by ABA and Ca^{2+} Is Impaired in *cpk8* and *cat3* Mutants.

(A) Representative whole-cell recordings of inward K^+ currents in guard cell protoplasts isolated from different materials (Col, *cpk8*, and *cat3*) with or without addition of 50 μM ABA in the bath solution. The voltage protocols, as well as time and current scale bars for the recordings, are shown inside the figure. Each trace represents the K^+ currents at the indicated voltage.

(B) Current density-voltage curves of steady state whole-cell inward K^+ currents in guard cell protoplasts isolated from different plant materials with or without the addition of 50 μM ABA in the bath solution. The data are derived from the recordings as shown in **(A)** and are presented as means ± SE (Col, $n = 12$; *cpk8*, $n = 11$; *cat3*, $n = 13$).

(C) Representative whole-cell recordings of inward K^+ currents in guard cell protoplasts isolated from different plant material (Col, *cpk8*, and *cat3*) with or without the addition of 2 μM free Ca^{2+} in pipette solution. The voltage protocols, as well as time and current scale bars for the recordings, are shown inside the figure. Each trace represents the K^+ currents at the indicated voltage.

(D) Current density-voltage curves of the steady state whole-cell inward K^+ currents in guard cell protoplasts isolated from different plant materials with or without the addition of 2 μM free Ca^{2+} in the pipette solution. The data are derived from the recordings as shown in **(C)** and are presented as means ± SE (Col, $n = 14$; Col+Ca^{2+}, $n = 21$; cpk8, $n = 13$; *cpk8*+Ca^{2+}, $n = 22$; *cat3*, $n = 15$; *cat3*+Ca^{2+}, $n = 20$).

identity. Previous studies have shown that several CDPKs play important roles in plant responses to drought and salt stresses (Saijo et al., 2000; Zhu et al., 2007; Xu et al., 2010; Zou et al., 2010; Latz et al., 2013). In this study, our results support the notion that CPK8 serves as a positive regulator in ABA-mediated stomatal movement in plant responses to drought stress (Figure 1). Hubbard et al. (2012) reported that ABA-induced stomatal closure is not significantly impaired in *cpk10*, *cpk4 cpk11*, and *cpk7 cpk8 cpk32* compared with wild-type plants, which was different from the findings of ABA insensitivity for *cpk4 cpk11* (Zhu et al., 2007), *cpk10* (Zou et al., 2010), and *cpk8* in this study (Figure 1H). The difference between these results may be due to the different protocols for stomatal aperture assay (Zhu et al., 2007; Zou et al., 2010; Hubbard et al., 2012).

Arabidopsis CDPKs display highly variable calcium dependences for their activities, and six CPKs (including CPK8) from subgroup 3 exhibit low or no calcium sensitivity (Boudsocq et al., 2012). CPK24 activity is independent of calcium, whereas Ca^{2+}-activated CPK11 subsequently phosphorylates CPK24, transducing the calcium signals and regulates SPIK activity during pollen tube growth (Zhao et al., 2013). CPK8 has weak calcium sensitivity (Boudsocq et al., 2012) and may

phosphorylate its substrate CAT3 even without addition of calcium in the reaction buffer (Figure 3A). However inhibition of the inward K^+ currents by Ca^{2+} (Figures 7C and 7D) was impaired in the *cpk8*, suggesting that CPK8 may function downstream of Ca^{2+}. These results indicate that CPK8 may be indirectly regulated by Ca^{2+} signals and that other Ca^{2+}-dependent proteins may transduce Ca^{2+} signals to CPK8. One example of a similar mechanism is Ca^{2+}-independent CPK24, which is activated (phosphorylated) by Ca^{2+}-dependent CPK11 (Zhao et al., 2013).

Ca^{2+}-Mediated Protein Phosphorylation: A Universal Regulatory Mechanism for Plant Ion channels and Transporters

A number of CDPKs have been reported to regulate ion channel activities in stomatal movement (Pei et al., 1996; Li et al., 1998; Mori et al., 2006; Geiger et al., 2010, 2011; Zou et al., 2010; Brandt et al., 2012; Scherzer et al., 2012), plant responses to salt stress (Latz et al., 2013), and pollen tube growth (Gutermuth et al., 2013; Zhao et al., 2013; Zhou et al., 2014). In this report, the plasma membrane localized-CPK8 showed abundant expression in stomatal guard cells (Figure 1D; Supplemental Figure 2), indicating its potential role in regulation of stomatal movement and ion channel activity. As shown in Figure 7, ABA and Ca^{2+} inhibition of inward K^+ currents were impaired in guard cells of *cpk8* mutant plants. So far, at least 11 Arabidopsis CDPKs have been reported to function in regulation of ion channel activity in plant cells (Hwang et al., 2000; Mori et al., 2006; Geiger et al., 2010, 2011; Zou et al., 2010; Brandt et al., 2012; Scherzer et al., 2012; Latz et al., 2013; Gutermuth et al., 2013; Zhao et al., 2013; Zhou et al., 2014). The previous reports have revealed that plant ion channels and transporters are regulated by members of the CIPK (CBL-interacting protein kinase) family, another Ca^{2+}-regulated protein kinase family, such as AKT1 regulation by CIPK23 (Xu et al., 2006; Wang and Wu, 2013) and Na^+/H^+ antiporter (SOS1) regulation by CIPK24 (Xiong et al., 2002). Together with the results in this study, these findings support the notion that regulation of various plant ion channels and transporters via their Ca^{2+}-mediated phosphorylation represents a universal mechanism.

Identification of a Downstream Target of CPK8

Identification and functional characterization of the specific target (or substrate) of a CDPK is a key step to understand CDPK functions in plant signaling (Boudsocq and Sheen, 2013). Some substrates of CDPKs have been identified in the last decade, revealing their different roles in plant development and immune and stress signaling (Boudsocq and Sheen, 2013; Schulz et al., 2013). For example, Arabidopsis CPK4 and CPK11 phosphorylate ABF1 and ABF4 during ABA signal transduction (Zhu et al., 2007). Arabidopsis CPK5 induces ROS production by directly phosphorylating the NADPH oxidase RBOHB during innate immune responses (Dubiella et al., 2013). Arabidopsis CPK11 and CPK24 modulate the activity of shaker pollen inward K^+ channel (SPIK, also named AKT6) during pollen tube growth (Zhao et al., 2013). In this study, yeast two-hybrid, co-IP, BiFC, and protein phosphorylation assays demonstrated specific interaction between CPK8 and CAT3 (Figures 2 and 3A). In addition, CPK8 specifically enhanced CAT3 activity through phosphorylation at Ser-261 (Figures 2 to 4). The *cpk8 cat3* double mutants showed similar drought stress sensitivity as the *cpk8* and *cat3* single mutants (Figure 6A). Similar to CPK8, CAT3 functions in the regulation of stomatal movement, most likely through regulation of the inward K^+ channel activities in stomatal guard cells (Figures 6D to 6F and 7). Our data reveal important roles of CPK8 and CAT3-mediated ABA stomatal signal transduction in response to drought stress.

Roles of CPK8-CAT3 Interaction in H_2O_2 Homeostasis

Excess ROS accumulation in living plant cells is toxic to cellular activities, so the cytosolic concentration of ROS must be stringently regulated (Mittler, 2002; Apel and Hirt, 2004). ROS play a dual role in plant responses to abiotic stresses, acting as toxic by-products of aerobic metabolism and as key regulators of growth, development, and defense pathways (Mittler et al., 2004; Miller et al., 2010). ROS-scavenging pathways are responsible for maintaining a low steady state level of ROS on which the different signals can be registered (Mittler et al., 2004; Miller et al., 2010). Rice (*Oryza sativa*) *CPK12*-overexpressing plants exhibit enhanced tolerance to salt stress, possibly as a result of decreased ROS accumulation (Asano et al., 2012). Arabidopsis glutathione peroxidase *GPX3* plays dual roles, the first in the general control of H_2O_2 homeostasis and the second in relaying ABA and H_2O_2 signaling in stomatal movement (Miao et al., 2006).

As an important H_2O_2-scavenging enzyme, the expression or activity of Arabidopsis catalase is also regulated by other components. The expression profiles and cellular localizations of Arabidopsis catalases are varied, suggesting their potential roles in response to environmental stimuli in addition to H_2O_2 decomposition (Zimmermann et al., 2006; Bueso et al., 2007; Xing et al., 2007; Du et al., 2008). ABA-induced *CAT1* expression depends on the production of H_2O_2, which is triggered by MKK1-MPK6 signaling pathway, revealing the roles of *CAT1* in ROS scavenging and its feedback regulation of the H_2O_2 signaling (Xing et al., 2007, 2008). *CAT2* has been reported to be involved in crosstalk between oxidative stress, cation homeostasis, and ethylene (Bueso et al., 2007). Arabidopsis CAT3 can interact with several proteins, such as CaM PCM6 in potato (*Solanum tuberosum*) (Yang and Poovaiah, 2002) and NDK1 (Fukamatsu et al., 2003), SOS2 (CIPK24; Verslues et al., 2007), and LSD1 (Li et al., 2013) in Arabidopsis, consistent with roles for CAT3 in regulating H_2O_2 homeostasis and signaling in response to ROS stress. This work showed that H_2O_2 can induce the expression of *CPK8* and *CAT3* (Supplemental Figures 1D and 5D). The *cpk8* and *cat3* mutants had lower catalase activities and accumulated more ROS in leaves and stomatal guard cells compared with wild-type plants when treated with ABA (Figures 5C to 5F), whereas *CPK8* and *CAT3* overexpression lines had lower ROS accumulation compared with wild-type plants when treated with ABA (Figures 5C and 5D).

In summary, the results presented in this study demonstrate that CPK8 can specifically phosphorylate CAT3 and regulate its activity. The CPK8-CAT3 interaction not only acts as a positive

regulatory component in ABA-mediated regulation of stomatal movement in plant responses to drought stress, but also plays important role in maintaining H_2O_2 homeostasis in living plant cells.

METHODS

Plant Materials and Growth Conditions

Arabidopsis thaliana ecotype Columbia and *Nicotiana benthamiana* were used in this study. The T-DNA insertion lines *cpk8* (SALK_036581) and *cat3* (SALK_092911) were obtained from the ABRC (http://www.arabidopsis.org/abrc/).

Seeds were surface sterilized and placed in the Petri dishes containing Murashige and Skoog agar (0.8%, w/v) medium and incubated for 2 d at 4°C before transfer to 22°C for germination. After 7 d under constant illumination at 60 μmol m^{-2} s^{-1} at 22°C, the seedlings were transplanted to pots containing soil mixture (rich soil:vermiculite, 2:1, v/v) and kept in growth chambers at 22°C with illumination at 120 μmol m^{-2} s^{-1} for a 16-h daily light period. The relative humidity was approximate 70% ($\pm$5%).

N. benthamiana seeds were planted in the potting soil mixture (rich soil: vermiculite, 2:1, v/v) and kept in growth chambers at 23°C with illumination at 120 μmol m^{-2} s^{-1} for a 16-h daily light period. After 3 weeks growth, the plants were used for transformation.

Vector Constructions and Generation of Transgenic Plants

The *$CPK8_{pro}$:GUS* construct was generated by introducing the *CPK8* promoter fragment (1.96 kb) in front of the *GUS* coding sequence in the *Eco*RI and *Sal*I sites of pCAMBIA1381 vector. The GUS staining assays were performed as described previously (Xu et al., 2006).

For *$Super_{pro}$:CPK8* and *$Super_{pro}$:CAT3* constructs, the coding sequence of *CPK8* was introduced into the *Kpn*I and *Xho*I sites of pCAMBIA1300 vector under the *Super* promoter, and the coding sequence of *CAT3* was introduced into the *Xba*I and *Xho*I sites of pCAMBIA1300 vector under the *Super* promoter (Chen et al., 2009), respectively. Primers for *$Super_{pro}$:CPK8* and *$Super_{pro}$:CAT3* constructs are listed in Supplemental Table 1. The *$Super_{pro}$:CPK8* and *$Super_{pro}$:CAT3* constructs were introduced into wild-type plants for generation of *CPK8* and *CAT3* overexpression lines, respectively. To generate the construct for complementation of *cpk8*, a genomic DNA fragment of *CPK8* was amplified and cloned into *Sac*I and *Kpn*I sites of pCAMBIA1300 vector. Arabidopsis transformation with *Agrobacterium tumefaciens* (strain GV3101) was performed by the floral dip method (Clough and Bent, 1998). Homozygous T3 transgenic lines were used for further analyses.

RT-qPCR

Total RNA was extracted from plants with Trizol reagent (Invitrogen) following the manufacturer's protocols. For RT-qPCR analyses, total RNA treated with DNase I (Takara) was used for cDNA synthesis by SuperScript II reverse transcriptase (Invitrogen). The quantitative PCR analysis was performed using an Applied Biosystems 7500 real-time PCR system. The SYBR Premix Ex Taq kit (Applied Biosystems) was used for reaction according to the manufacturer's instruction. Arabidopsis *18S rRNA* was quantified as an internal control. The primer sequences of *CPK8, CAT3* and *18S rRNA* for RT-qPCR are listed in Supplemental Table 1.

Drought Treatment and Water Loss Measurements

For drought treatment, plants grown on Murashige and Skoog medium for 7 d were transplanted into soil for about 1 week with sufficient watering followed by a 20-d drought stress (withholding irrigation) as described before (Zou et al., 2010), with slight modifications. The seedlings were grown in a growth room with 12-h daily light. Normally watered plants were used as the control. For drought stress treatment, water was withheld for 20 d (normal drought stress) or 22 d (severe drought stress). Two independent transgenic lines were used for drought stress.

For water loss measurement, rosette leaves were detached from 4-week-old plants, weighed, and placed on the laboratory bench (the relative humidity was between 40 and 50%) at 22°C ($\pm$1°C). Weight loss of the detached leaves was monitored at the indicated time intervals. Water loss was expressed as the percentage of initial fresh weight.

Thermal Imaging

Thermal imaging of plants was performed as described previously (Hua et al., 2012). Three-week-old plants grown under normal conditions were subjected to drought stress for about 1 week. Thermal images were obtained using VarioCAM HD and leaf temperature was calculated using IRBIS 3 software.

Stomatal Aperture Measurements

Stomatal closure assays were conducted as described before (Zou et al., 2010). After treatment, the abaxial epidermis was peeled and photographed using a Leica microscope (Leica DFC320). Stomatal apertures were measured using ImageJ software (National Institutes of Health).

Yeast Two-Hybrid Assay

The GAL4-based two-hybrid system was used for yeast two-hybrid screening (Clontech). The CPK8-pGBKT7 construct was generated by fusing the sequence encoding the CPK8 kinase domain (from 169 to 945 bp of the coding sequence) with that encoding the GAL4 binding domain in the *Eco*RI and *Sal*I sites of pGBKT7, and the resulting construct was transformed into the AH109 yeast strain. For screening, the reporter yeast was transformed with library plasmid DNA from CD4-22 library (ABRC). Yeast transformation, growth conditions, and assays for β-gal activity were performed according to the manufacturer's instructions (Clontech). Positive clones were selected for sequencing. Three coding sequences of catalases were inserted into pGADT7 prey plasmid containing the GAL4 activating domain and cotransformed into AH109 with CPK8 bait for β-gal activity assays, respectively. The primer sequences and restriction sites are listed in Supplemental Table 1.

Co-IP Assays

The coding sequence of *CPK8* with a cMyc tag (cMYC-CPK8) was cloned into the *Spe*I and *Kpn*I sites of pCAMBIA1307 vector under control of the *35S* promoter. The coding sequence of *CAT3* with a GFP tag (GFP-CAT3) was cloned into the *Xba*I and *Sal*I sites of pSAT6-GFP-N1 vector under control of the *35S* promoter. The primer sequences and restriction sites are listed in Supplemental Table 1. The combinations of cMyc-CPK8 and GFP-CAT3 were cotransformed into Arabidopsis mesophyll protoplasts as described before (Ren et al., 2013). After incubation overnight at 4°C, the protoplasts were lysed, sonicated, and centrifuged at 12,000*g* for 10 min at 4°C. The supernatant was incubated with 10 μL anti-cMyc agarose conjugate (Sigma-Aldrich) for 6 h at 4°C. The co-IP products were washed briefly with extraction buffer for five times at 4°C and then detected via immunoblot analysis. Both anti-GFP (Sigma-Aldrich) and anti-cMyc (Sigma-Aldrich) antibodies were used at 1:5000 dilutions, and chemiluminescence signals were detected using Fusion Solo.

Subcellular Localizations of CPK8 and CAT3

For generation of GFP-fusion protein, the coding sequence of *CPK8* was fused with *GFP* in the *Xba*I and *Kpn*I sites of pCAMBIA1300 vector. The

coding sequence of *CAT3* was fused with *GFP* in the *Asc*I and *Pac*I sites of pCM1205-C-GFP vector (Zhou et al., 2012). The coding sequence for potassium transporter AKT1 (Xu et al., 2006) was fused with *mCherry* in the SUPERR:sXVE:mCherry$_C$:Bar vector (Schlücking et al., 2013) and used as the plasma membrane marker. PX-RK (CD3-83; ABRC) was used as peroxisome marker. All constructs were transformed into the Agrobacterium strain GV3101. The Agrobacterium lines were infiltrated into leaves of *N. benthamiana*. Plants were grown at 23°C and allowed to recover for 3 d. The fluorescence of GFP or mCherry in the leaves was imaged using a confocal laser scanning microscope (Leica sp5).

BiFC Assays

BiFC assays were performed as described previously (Waadt and Kudla, 2008). For generation of the BiFC vectors, the coding region of *CPK8* was cloned via *Bam*HI-*Sal*I into pSPYCEM, resulting in CPK8-YC, and the coding region of *CAT1*, *CAT2*, or *CAT3* was cloned via *Bam*HI-*Sal*I into pSPYNE173, resulting in CAT1-YN, CAT2-YN and CAT3-YN, respectively. The gene-specific primer pairs for *CPK8* and *CATs* are listed in Supplemental Table 1. All constructs were transformed into the Agrobacterium strain GV3101. An equal volume of Agrobacterium harboring CPK8-YC, CAT1-YN (or CAT2-YN, CAT3-YN) and P19 was mixed to a final concentration of OD_{600} = 0.8. Agrobacterium lines were infiltrated leaves of *N. benthamiana*. Plants were grown at 23°C and allowed to recover for 3 d; then, the fluorescence of YFP in the leaves was imaged using a confocal laser scanning microscope (Leica sp5).

Firefly Luciferase Complementation Image Assay

Firefly luciferase complementation imaging assays were performed as described before (Chen et al., 2008). For generation of the assay vectors, the coding region of *CPK8* was cloned via *Bam*HI-*Sal*I into pCAMBIA1300-cLuc, resulting in CPK8-CLuc, and the coding region of *CAT1*, *CAT2*, or *CAT3* was cloned via *Bam*HI-*Sal*I into pCAMBIA1300-nLuc, resulting in CAT1-nLuc, CAT2-nLuc, or CAT3-nLuc, respectively. The gene-specific primer pairs for *CPK8* and *CATs* are shown in Supplemental Table 1.

All constructs were transformed into the Agrobacterium strain GV3101. An equal volume of Agrobacterium harboring pCAMBIA-nLuc, pCAMBIA-cLuc, and P19 was mixed to a final concentration of OD_{600} = 0.8. Three different combinations of Agrobacterium were infiltrated into three different positions at the same leaves of *N. benthamiana*. Plants were grown at 23°C and allowed to recover for 3 d. A low-light cooled CCD imaging apparatus (fluorescence/chemiluminescence imaging system) was used to capture the LUC image.

In Vitro Kinase Assay

To prepare recombinant CPK8, the full-length coding sequence of *CPK8* was amplified and cloned into the *Xcm*I sites of pCXSN vector, resulting in pCXSN-Strep-CPK8. The gene-specific primer pairs of *CPK8* are listed in Supplemental Table 1. The Strep-CPK8 was purified as described previously (Witte et al., 2004).

To prepare recombinant CAT1, CAT2, and CAT3 truncated proteins, the corresponding coding sequences of *CATs* were amplified and cloned into *Bam*HI and *Sal*I sites of pGEX-4T-1 vector, resulting in pGEX-4T-1-CATs constructs, respectively. CAT3 mutant proteins were made by site-directed mutagenesis using a QuickChange kit (Agilent Technologies; the primers are listed in Supplemental Table 1). The constructs were then introduced into BL21 cells by transformation and used to purify GST-CAT proteins.

In vitro kinase assays were performed as described previously (Rodriguez Milla et al., 2006), with slight modification. In brief, phosphorylation was initiated by adding 0.5 μCi [γ-^{32}P] to reaction buffer containing 25 mM Tris-HCl (pH 7.5), 10 mM $MgCl_2$, 1 mM DTT, and 10 μM ATP, followed by incubation for 20 min at 25°C. The proteins were separated by 10% SDS-PAGE, and the phosphorylated proteins were visualized by autoradiography.

In Planta Kinase Assay

In planta kinase assays were used to test the phosphorylation of CAT3. Total proteins in Col/35S$_{pro}$:CAT3-GFP or *cpk8*/35S$_{pro}$:CAT3-GFP before and after treatment with ABA were extracted. CAT3-GFP proteins were immunoprecipitated using Anti-GFP mAb agarose (MBL). CAT3-GFP proteins were then separated by 10% SDS-PAGE, and phosphorylated proteins were detected by immunoblotting using Biotinylated Phos-tag as described previously (Kinoshita-Kikuta et al., 2007). Calf intestinal alkaline phosphatase-treated (Takara) proteins were used as control.

Measurements of H_2O_2 Production

H_2O_2 was detected by DAB staining as described previously (Thordal-Christensen et al., 1997; Guan and Scandalios, 2000). Fully expanded leaves were excised and incubated in water containing 100 μM ABA for 30 min in dark at 28°C. The leaves were then incubated in DAB solution (1 mg mL^{-1}, pH 3.8; Sigma-Aldrich) for 8 h in dark at 28°C. The leaves were immersed in boiling 80% (v/v) ethanol for 10 min to terminate the staining and to decolor the leaves (except for the deep brown polymerization product produced by the reaction of DAB with H_2O_2). After cooling, the leaves were extracted with 80% (v/v) ethanol and preserved at 4°C in 80% (v/v) ethanol before photographed.

ROS production in guard cells was examined by loading abaxial epidermal strips with H_2DCF-DA (Miao et al., 2006). The detached leaves were floated in incubation buffer for 2.5 h to induce stomatal opening, and the epidermal strips were peeled and placed into loading buffer (10 mM Tris and 50 mM KCl, pH 7.2) containing 50 μM H_2DCF-DA in the dark for 10 min. Excess dye was removed by washing the samples three times with distilled water. Epidermal tissues were then incubated in loading buffer for 5 min with 50 μM ABA or with an equal volume of ethanol added as a control. Examinations of peel fluorescence were performed with a confocal laser scanning microscope (Nikon TE2000-E). To quantitatively analyze the data, pixel values were averaged over rectangular regions (4 μm^2) manually located on each image. The pixel intensity from at least 150 guard cells was recorded.

Measurement of Catalase Activity

The activity of CAT was determined with a CAT assay kit according to the manufacturer's instructions (Beyotime). Briefly, samples were treated with excess H_2O_2 for decomposition by catalase for 5 min, and the remaining H_2O_2 coupled with a substrate was treated with peroxidase to generate a red product, *N*-4-antipyryl-3-chloro-5-sulfonate-*p*-benzoquinonemonoimine, which absorbs maximally at 520 nm. Catalase activity was thus determined by measuring the decomposed H_2O_2. All values were normalized by the total protein concentration of the same sample.

Patch-Clamp Experiments

Arabidopsis guard cell protoplasts were isolated as described previously (Pei et al., 1997; Wang et al., 2001). Standard whole-cell recording techniques were applied in this study (Hamill et al., 1981). All experiments were conducted at room temperature (~22°C) under dim light. The whole-cell currents were recorded as described before (Zou et al., 2010). The pCLAMP software (version 6.0.4; Axon Instruments) was used to acquire and analyze the whole-cell currents. SigmaPlot software was used to draw current-voltage plots and for data analysis.

Accession Numbers

Sequence data from this article can be found in the Arabidopsis Genome Initiative or GenBank/EMBL databases under the following accession numbers: At5g19450 for *CPK8*, At1g20630 for *CAT1*, At4g35090 for *CAT2*, and At1g20620 for *CAT3*.

Supplemental Data

Supplemental Figure 1. Position of T-DNA Insertion in *cpk8* and Expression Levels of *CPK8* in Response to Abiotic Stresses.

Supplemental Figure 2. Subcellular Localizations of CPK8 and CAT3.

Supplemental Figure 3. Firefly Luciferase Complementation Image Assay of CPK8 Interaction with CAT3 in *N. benthamiana* Leaves.

Supplemental Figure 4. Identification of CPK8 Phosphorylation Sites in CAT3.

Supplemental Figure 5. Position of T-DNA Insertion in *CAT3* and Expression Levels of *CAT3* in Response to ABA and H_2O_2.

Supplemental Figure 6. Phenotype Observation of Various *CPK8*- and *CAT3*-Related Plant Materials under Drought Stress.

Supplemental Figure 7. ABA Inhibition of Stomatal Opening Is Impaired in the *cpk8* and *cat3* Mutants.

Supplemental Figure 8. Expression Patterns of *CPK7* as Determined from $CPK7_{pro}$*:GUS* Transgenic Plants.

Supplemental Table 1. Primer Sequences Used in This Study.

ACKNOWLEDGMENTS

This work was financially supported by grants from the "973" Project (2011CB915401 and 2012CB114203 to W.-H.W.), the "111" Project (No. B06003 to W.-H.W.), and the National Natural Science Foundation of China (31000119 to J.-J.Z.). We thank Jörg Kudla (Institut für Botanik, Universität Münster, Germany) for providing the vectors SUPERR:sXVE: $mCherry_C$:Bar for AKT1-mCherry construct and pSPYCEM and pSPYNE173 for BiFC assays. We thank Yan Guo (China Agricultural University) for providing pCM1205-C-GFP and pSAT6-GFP-N1 vectors.

AUTHOR CONTRIBUTIONS

J.-J.Z. and W.-H.W. designed the research. J.-J.Z., D.R., X.-D.L., C.W., W.-X.L., L.-F.S., and W.-Z.Z. performed research and analyzed data. J.-Z.Z. and W.-H.W. wrote the article. J.-J.Z., X.-D.L., and W.-H.W. revised the article.

Received February 15, 2015; revised April 11, 2015; accepted April 23, 2015; published May 12, 2015.

REFERENCES

Apel, K., and Hirt, H. (2004). Reactive oxygen species: metabolism, oxidative stress, and signal transduction. Annu. Rev. Plant Biol. **55:** 373–399.

Asano, T., Hayashi, N., Kobayashi, M., Aoki, N., Miyao, A., Mitsuhara, I., Ichikawa, H., Komatsu, S., Hirochika, H., Kikuchi, S., and Ohsugi, R. (2012). A rice calcium-dependent protein kinase OsCPK12 oppositely modulates salt-stress tolerance and blast disease resistance. Plant J. **69:** 26–36.

Böhmer, M., and Romeis, T. (2007). A chemical-genetic approach to elucidate protein kinase function in *planta.* Plant Mol. Biol. **65:** 817–827.

Blatt, M.R. (1990). Potassium channel currents in intact stomatal guard cells: rapid enhancement by abscisic acid. Planta **180:** 445–455.

Boudsocq, M., Droillard, M.J., Regad, L., and Laurière, C. (2012). Characterization of *Arabidopsis* calcium-dependent protein kinases: activated or not by calcium? Biochem. J. **447:** 291–299.

Boudsocq, M., and Sheen, J. (2013). CDPKs in immune and stress signaling. Trends Plant Sci. **18:** 30–40.

Boudsocq, M., Willmann, M.R., McCormack, M., Lee, H., Shan, L., He, P., Bush, J., Cheng, S.H., and Sheen, J. (2010). Differential innate immune signalling via $Ca^{(2+)}$ sensor protein kinases. Nature **464:** 418–422.

Brandt, B., Brodsky, D.E., Xue, S., Negi, J., Iba, K., Kangasjärvi, J., Ghassemian, M., Stephan, A.B., Hu, H., and Schroeder, J.I. (2012). Reconstitution of abscisic acid activation of SLAC1 anion channel by CPK6 and OST1 kinases and branched ABI1 PP2C phosphatase action. Proc. Natl. Acad. Sci. USA **109:** 10593–10598.

Bueso, E., Alejandro, S., Carbonell, P., Perez-Amador, M.A., Fayos, J., Bellés, J.M., Rodriguez, P.L., and Serrano, R. (2007). The lithium tolerance of the Arabidopsis *cat2* mutant reveals a cross-talk between oxidative stress and ethylene. Plant J. **52:** 1052–1065.

Chen, H., Zou, Y., Shang, Y., Lin, H., Wang, Y., Cai, R., Tang, X., and Zhou, J.M. (2008). Firefly luciferase complementation imaging assay for protein-protein interactions in plants. Plant Physiol. **146:** 368–376.

Cheng, S.-H., Willmann, M.R., Chen, H.-C., and Sheen, J. (2002). Calcium signaling through protein kinases. The Arabidopsis calcium-dependent protein kinase gene family. Plant Physiol. **129:** 469–485.

Chen, Y.-F., Li, L.-Q., Xu, Q., Kong, Y.-H., Wang, H., and Wu, W.-H. (2009). The WRKY6 transcription factor modulates *PHOSPHATE1* expression in response to low Pi stress in *Arabidopsis.* Plant Cell **21:** 3554–3566.

Choi, H.I., Park, H.-J., Park, J.H., Kim, S., Im, M.-Y., Seo, H.-H., Kim, Y.-W., Hwang, I., and Kim, S.Y. (2005). Arabidopsis calcium-dependent protein kinase AtCPK32 interacts with ABF4, a transcriptional regulator of abscisic acid-responsive gene expression, and modulates its activity. Plant Physiol. **139:** 1750–1761.

Clough, S.J., and Bent, A.F. (1998). Floral dip: a simplified method for *Agrobacterium*-mediated transformation of *Arabidopsis thaliana.* Plant J. **16:** 735–743.

Coca, M., and San Segundo, B. (2010). AtCPK1 calcium-dependent protein kinase mediates pathogen resistance in Arabidopsis. Plant J. **63:** 526–540.

Dammann, C., Ichida, A., Hong, B., Romanowsky, S.M., Hrabak, E.M., Harmon, A.C., Pickard, B.G., and Harper, J.F. (2003). Subcellular targeting of nine calcium-dependent protein kinase isoforms from Arabidopsis. Plant Physiol. **132:** 1840–1848.

Du, Y.-Y., Wang, P.-C., Chen, J., and Song, C.-P. (2008). Comprehensive functional analysis of the catalase gene family in *Arabidopsis thaliana.* J. Integr. Plant Biol. **50:** 1318–1326.

Dubiella, U., Seybold, H., Durian, G., Komander, E., Lassig, R., Witte, C.-P., Schulze, W.X., and Romeis, T. (2013). Calcium-dependent protein kinase/NADPH oxidase activation circuit is required for rapid defense signal propagation. Proc. Natl. Acad. Sci. USA **110:** 8744–8749.

Franz, S., Ehlert, B., Liese, A., Kurth, J., Cazalé, A.-C., and Romeis, T. (2011). Calcium-dependent protein kinase CPK21 functions in abiotic stress response in *Arabidopsis thaliana.* Mol. Plant **4:** 83–96.

Frugoli, J.A., Zhong, H.H., Nuccio, M.L., McCourt, P., McPeek, M.A., Thomas, T.L., and McClung, C.R. (1996). Catalase is

encoded by a multigene family in *Arabidopsis thaliana* (L.) Heynh. Plant Physiol. **112:** 327–336.

Fukamatsu, Y., Yabe, N., and Hasunuma, K. (2003). *Arabidopsis* NDK1 is a component of ROS signaling by interacting with three catalases. Plant Cell Physiol. **44:** 982–989.

Geiger, D., Scherzer, S., Mumm, P., Marten, I., Ache, P., Matschi, S., Liese, A., Wellmann, C., Al-Rasheid, K.A.S., Grill, E., Romeis, T., and Hedrich, R. (2010). Guard cell anion channel SLAC1 is regulated by CDPK protein kinases with distinct Ca^{2+} affinities. Proc. Natl. Acad. Sci. USA **107:** 8023–8028.

Geiger, D., Maierhofer, T., Al-Rasheid, K.A., Scherzer, S., Mumm, P., Liese, A., Ache, P., Wellmann, C., Marten, I., Grill, E., Romeis, T., and Hedrich, R. (2011). Stomatal closure by fast abscisic acid signaling is mediated by the guard cell anion channel SLAH3 and the receptor RCAR1. Sci. Signal. **4:** ra32.

Grabov, A., and Blatt, M.R. (1997). Parallel control of the inward-rectifier K^+ channel by cytosolic free Ca^{2+} and pH in *Vicia* guard cells. Planta **201:** 84–95.

Grabov, A., and Blatt, M.R. (1999). A steep dependence of inward-rectifying potassium channels on cytosolic free calcium concentration increase evoked by hyperpolarization in guard cells. Plant Physiol. **119:** 277–288.

Guan, L.M., and Scandalios, J.G. (2000). Hydrogen-peroxide-mediated catalase gene expression in response to wounding. Free Radic. Biol. Med. **28:** 1182–1190.

Gutermuth, T., Lassig, R., Portes, M.T., Maierhofer, T., Romeis, T., Borst, J.W., Hedrich, R., Feijó, J.A., and Konrad, K.R. (2013). Pollen tube growth regulation by free anions depends on the interaction between the anion channel SLAH3 and calcium-dependent protein kinases CPK2 and CPK20. Plant Cell **25:** 4525–4543.

Hamill, O.P., Marty, A., Neher, E., Sakmann, B., and Sigworth, F.J. (1981). Improved patch-clamp techniques for high-resolution current recording from cells and cell-free membrane patches. Pflugers Arch. **391:** 85–100.

Harmon, A.C., Gribskov, M., and Harper, J.F. (2000). CDPKs - a kinase for every Ca^{2+} signal? Trends Plant Sci. **5:** 154–159.

Harper, J.F., and Harmon, A. (2005). Plants, symbiosis and parasites: a calcium signalling connection. Nat. Rev. Mol. Cell Biol. **6:** 555–566.

Harper, J.F., Breton, G., and Harmon, A. (2004). Decoding $Ca^{(2+)}$ signals through plant protein kinases. Annu. Rev. Plant Biol. **55:** 263–288.

Hua, D., Wang, C., He, J., Liao, H., Duan, Y., Zhu, Z., Guo, Y., Chen, Z., and Gong, Z. (2012). A plasma membrane receptor kinase, GHR1, mediates abscisic acid- and hydrogen peroxide-regulated stomatal movement in Arabidopsis. Plant Cell **24:** 2546–2561.

Hubbard, K.E., Siegel, R.S., Valerio, G., Brandt, B., and Schroeder, J.I. (2012). Abscisic acid and CO_2 signalling via calcium sensitivity priming in guard cells, new CDPK mutant phenotypes and a method for improved resolution of stomatal stimulus-response analyses. Ann. Bot. (Lond.) **109:** 5–17.

Hwang, I., Sze, H., and Harper, J.F. (2000). A calcium-dependent protein kinase can inhibit a calmodulin-stimulated Ca^{2+} pump (ACA2) located in the endoplasmic reticulum of Arabidopsis. Proc. Natl. Acad. Sci. USA **97:** 6224–6229.

Ivashikina, N., Deeken, R., Fischer, S., Ache, P., and Hedrich, R. (2005). AKT2/3 subunits render guard cell K^+ channels Ca^{2+} sensitive. J. Gen. Physiol. **125:** 483–492.

Jannat, R., Uraji, M., Morofuji, M., Islam, M.M., Bloom, R.E., Nakamura, Y., McClung, C.R., Schroeder, J.I., Mori, I.C., and Murata, Y. (2011). Roles of intracellular hydrogen peroxide accumulation in abscisic acid signaling in *Arabidopsis* guard cells. J. Plant Physiol. **168:** 1919–1926.

Kanchiswamy, C.N., et al. (2010). Regulation of Arabidopsis defense responses against *Spodoptera littoralis* by CPK-mediated calcium signaling. BMC Plant Biol. **10:** 97.

Kelly, W.B., Esser, J.E., and Schroeder, J.I. (1995). Effects of cytosolic calcium and limited, possible dual, effects of G protein modulators on guard cell inward potassium channels. Plant J. **8:** 479–489.

Kinoshita-Kikuta, E., Aoki, Y., Kinoshita, E., and Koike, T. (2007). Label-free kinase profiling using phosphate affinity polyacrylamide gel electrophoresis. Mol. Cell. Proteomics **6:** 356–366.

Kolukisaoglu, U., Weinl, S., Blazevic, D., Batistic, O., and Kudla, J. (2004). Calcium sensors and their interacting protein kinases: genomics of the Arabidopsis and rice CBL-CIPK signaling networks. Plant Physiol. **134:** 43–58.

Kudla, J., Batistič, O., and Hashimoto, K. (2010). Calcium signals: the lead currency of plant information processing. Plant Cell **22:** 541–563.

Kwak, J.M., Mori, I.C., Pei, Z.M., Leonhardt, N., Torres, M.A., Dangl, J.L., Bloom, R.E., Bodde, S., Jones, J.D., and Schroeder, J.I. (2003). NADPH oxidase *AtrbohD* and *AtrbohF* genes function in ROS-dependent ABA signaling in *Arabidopsis.* EMBO J. **22:** 2623–2633.

Latz, A., Mehlmer, N., Zapf, S., Mueller, T.D., Wurzinger, B., Pfister, B., Csaszar, E., Hedrich, R., Teige, M., and Becker, D. (2013). Salt stress triggers phosphorylation of the Arabidopsis vacuolar K^+ channel TPK1 by calcium-dependent protein kinases (CDPKs). Mol. Plant **6:** 1274–1289.

Lee, S.S., Cho, H.S., Yoon, G.M., Ahn, J.W., Kim, H.H., and Pai, H.S. (2003). Interaction of NtCDPK1 calcium-dependent protein kinase with NtRpn3 regulatory subunit of the 26S proteasome in *Nicotiana tabacum.* Plant J. **33:** 825–840.

Li, G., Boudsocq, M., Hem, S., Vialaret, J., Rossignol, M., Maurel, C., and Santoni, V. (2014). The calcium-dependent protein kinase CPK7 acts on root hydraulic conductivity. Plant Cell Environ., 10.1111/pce.12478.

Li, J., Lee, Y.-R.J., and Assmann, S.M. (1998). Guard cells possess a calcium-dependent protein kinase that phosphorylates the KAT1 potassium channel. Plant Physiol. **116:** 785–795.

Li, Y., Chen, L., Mu, J., and Zuo, J. (2013). LESION SIMULATING DISEASE1 interacts with catalases to regulate hypersensitive cell death in Arabidopsis. Plant Physiol. **163:** 1059–1070.

Luan, S. (2009). The CBL-CIPK network in plant calcium signaling. Trends Plant Sci. **14:** 37–42.

Luan, S., Kudla, J., Rodriguez-Concepcion, M., Yalovsky, S., and Gruissem, W. (2002). Calmodulins and calcineurin B-like proteins: calcium sensors for specific signal response coupling in plants. Plant Cell **14** (Suppl)**:** S389–S400.

Ludwig, A.A., Romeis, T., and Jones, J.D.G. (2004). CDPK-mediated signalling pathways: specificity and cross-talk. J. Exp. Bot. **55:** 181–188.

Matschi, S., Werner, S., Schulze, W.X., Legen, J., Hilger, H.H., and Romeis, T. (2013). Function of calcium-dependent protein kinase CPK28 of *Arabidopsis thaliana* in plant stem elongation and vascular development. Plant J. **73:** 883–896.

McCormack, E., Tsai, Y.-C., and Braam, J. (2005). Handling calcium signaling: *Arabidopsis* CaMs and CMLs. Trends Plant Sci. **10:** 383–389.

Mehlmer, N., Wurzinger, B., Stael, S., Hofmann-Rodrigues, D., Csaszar, E., Pfister, B., Bayer, R., and Teige, M. (2010). The Ca^{2+}-dependent protein kinase CPK3 is required for MAPK-independent salt-stress acclimation in Arabidopsis. Plant J. **63:** 484–498.

Mhamdi, A., Queval, G., Chaouch, S., Vanderauwera, S., Van Breusegem, F., and Noctor, G. (2010). Catalase function in plants: a focus on *Arabidopsis* mutants as stress-mimic models. J. Exp. Bot. **61:** 4197–4220.

Miao, Y., Lv, D., Wang, P., Wang, X.-C., Chen, J., Miao, C., and Song, C.-P. (2006). An Arabidopsis glutathione peroxidase

functions as both a redox transducer and a scavenger in abscisic acid and drought stress responses. Plant Cell **18:** 2749–2766.

Miller, G., Suzuki, N., Ciftci-Yilmaz, S., and Mittler, R. (2010). Reactive oxygen species homeostasis and signalling during drought and salinity stresses. Plant Cell Environ. **33:** 453–467.

Mittler, R. (2002). Oxidative stress, antioxidants and stress tolerance. Trends Plant Sci. **7:** 405–410.

Mittler, R., Vanderauwera, S., Gollery, M., and Van Breusegem, F. (2004). Reactive oxygen gene network of plants. Trends Plant Sci. **9:** 490–498.

Mori, I.C., Murata, Y., Yang, Y., Munemasa, S., Wang, Y.-F., Andreoli, S., Tiriac, H., Alonso, J.M., Harper, J.F., Ecker, J.R., Kwak, J.M., and Schroeder, J.I. (2006). CDPKs CPK6 and CPK3 function in ABA regulation of guard cell S-type anion- and $Ca^{(2+)}$-permeable channels and stomatal closure. PLoS Biol. **4:** e327.

Murata, Y., Pei, Z.-M., Mori, I.C., and Schroeder, J. (2001). Abscisic acid activation of plasma membrane Ca^{2+} channels in guard cells requires cytosolic NAD(P)H and is differentially disrupted upstream and downstream of reactive oxygen species production in *abi1-1* and *abi2-1* protein phosphatase 2C mutants. Plant Cell **13:** 2513–2523.

Myers, C., Romanowsky, S.M., Barron, Y.D., Garg, S., Azuse, C.L., Curran, A., Davis, R.M., Hatton, J., Harmon, A.C., and Harper, J.F. (2009). Calcium-dependent protein kinases regulate polarized tip growth in pollen tubes. Plant J. **59:** 528–539.

Patharkar, O.R., and Cushman, J.C. (2000). A stress-induced calcium-dependent protein kinase from *Mesembryanthemum crystallinum* phosphorylates a two-component pseudo-response regulator. Plant J. **24:** 679–691.

Pei, Z.M., Kuchitsu, K., Ward, J.M., Schwarz, M., and Schroeder, J.I. (1997). Differential abscisic acid regulation of guard cell slow anion channels in Arabidopsis wild-type and *abi1* and *abi2* mutants. Plant Cell **9:** 409–423.

Pei, Z.-M., Murata, Y., Benning, G., Thomine, S., Klüsener, B., Allen, G.J., Grill, E., and Schroeder, J.I. (2000). Calcium channels activated by hydrogen peroxide mediate abscisic acid signalling in guard cells. Nature **406:** 731–734.

Pei, Z.M., Ward, J.M., Harper, J.F., and Schroeder, J.I. (1996). A novel chloride channel in *Vicia faba* guard cell vacuoles activated by the serine/threonine kinase, CDPK. EMBO J. **15:** 6564–6574.

Reiland, S., Messerli, G., Baerenfaller, K., Gerrits, B., Endler, A., Grossmann, J., Gruissem, W., and Baginsky, S. (2009). Large-scale Arabidopsis phosphoproteome profiling reveals novel chloroplast kinase substrates and phosphorylation networks. Plant Physiol. **150:** 889–903.

Ren, X.L., Qi, G.N., Feng, H.Q., Zhao, S., Zhao, S.S., Wang, Y., and Wu, W.H. (2013). Calcineurin B-like protein CBL10 directly interacts with AKT1 and modulates K^+ homeostasis in Arabidopsis. Plant J. **74:** 258–266.

Rodriguez Milla, M.A., Uno, Y., Chang, I.-F., Townsend, J., Maher, E.A., Quilici, D., and Cushman, J.C. (2006). A novel yeast two-hybrid approach to identify CDPK substrates: characterization of the interaction between AtCPK11 and AtDi19, a nuclear zinc finger protein. FEBS Lett. **580:** 904–911.

Romeis, T., and Herde, M. (2014). From local to global: CDPKs in systemic defense signaling upon microbial and herbivore attack. Curr. Opin. Plant Biol. **20:** 1–10.

Saijo, Y., Hata, S., Kyozuka, J., Shimamoto, K., and Izui, K. (2000). Over-expression of a single Ca^{2+}-dependent protein kinase confers both cold and salt/drought tolerance on rice plants. Plant J. **23:** 319–327.

Schroeder, J.I., and Hagiwara, S. (1989). Cytosolic calcium regulates ion channels in the plasma membrane of *Vicia faba* guard cells. Nature **338:** 427–430.

Schroeder, J.I., Allen, G.J., Hugouvieux, V., Kwak, J.M., and Waner, D. (2001). Guard cell signal transduction. Annu. Rev. Plant Physiol. Plant Mol. Biol. **52:** 627–658.

Scherzer, S., Maierhofer, T., Al-Rasheid, K.A., Geiger, D., and Hedrich, R. (2012). Multiple calcium-dependent kinases modulate ABA-activated guard cell anion channels. Mol. Plant **5:** 1409–1412.

Schlücking, K., Edel, K.H., Köster, P., Drerup, M.M., Eckert, C., Steinhorst, L., Waadt, R., Batistič, O., and Kudla, J. (2013). A new beta-estradiol-inducible vector set that facilitates easy construction and efficient expression of transgenes reveals CBL3-dependent cytoplasm to tonoplast translocation of CIPK5. Mol. Plant **6:** 1814–1829.

Schulz, P., Herde, M., and Romeis, T. (2013). Calcium-dependent protein kinases: hubs in plant stress signaling and development. Plant Physiol. **163:** 523–530.

Schwartz, A., Wu, W.H., Tucker, E.B., and Assmann, S.M. (1994). Inhibition of inward K^+ channels and stomatal response by abscisic acid: an intracellular locus of phytohormone action. Proc. Natl. Acad. Sci. USA **91:** 4019–4023.

Shao, J., and Harmon, A.C. (2003). *In vivo* phosphorylation of a recombinant peptide substrate of CDPK suggests involvement of CDPK in plant stress responses. Plant Mol. Biol. **53:** 691–700.

Thordal-Christensen, H., Zhang, Z., Wei, Y., and Collinge, D.B. (1997). Subcellular localization of H_2O_2 in plants. H_2O_2 accumulation in papillae and hypersensitive response during the barley-powdery mildew interaction. Plant J. **11:** 1187–1194.

Uno, Y., Rodriguez Milla, M.A., Maher, E., and Cushman, J.C. (2009). Identification of proteins that interact with catalytically active calcium-dependent protein kinases from *Arabidopsis.* Mol. Genet. Genomics **281:** 375–390.

Verslues, P.E., Batelli, G., Grillo, S., Agius, F., Kim, Y.-S., Zhu, J., Agarwal, M., Katiyar-Agarwal, S., and Zhu, J.-K. (2007). Interaction of SOS2 with nucleoside diphosphate kinase 2 and catalases reveals a point of connection between salt stress and H_2O_2 signaling in *Arabidopsis thaliana.* Mol. Cell. Biol. **27:** 7771–7780.

Vlad, F., Turk, B.E., Peynot, P., Leung, J., and Merlot, S. (2008). A versatile strategy to define the phosphorylation preferences of plant protein kinases and screen for putative substrates. Plant J. **55:** 104–117.

Waadt, R., and Kudla, J. (2008). *In planta* visualization of protein interactions using bimolecular fluorescence complementation (BiFC). CSH Protoc. **2008:** prot4995.

Wang, X.-Q., Ullah, H., Jones, A.M., and Assmann, S.M. (2001). G protein regulation of ion channels and abscisic acid signaling in *Arabidopsis* guard cells. Science **292:** 2070–2072.

Wang, Y., and Wu, W.H. (2013). Potassium transport and signaling in higher plants. Annu. Rev. Plant Biol. **64:** 451–476.

Weinl, S., and Kudla, J. (2009). The CBL-CIPK Ca^{2+}-decoding signaling network: function and perspectives. New Phytol. **184:** 517–528.

White, P.J., and Broadley, M.R. (2003). Calcium in plants. Ann. Bot. (Lond.) **92:** 487–511.

Witte, C.P., Noël, L.D., Gielbert, J., Parker, J.E., and Romeis, T. (2004). Rapid one-step protein purification from plant material using the eight-amino acid StrepII epitope. Plant Mol. Biol. **55:** 135–147.

Xing, Y., Jia, W., and Zhang, J. (2007). AtMEK1 mediates stress-induced gene expression of CAT1 catalase by triggering H_2O_2 production in *Arabidopsis.* J. Exp. Bot. **58:** 2969–2981.

Xing, Y., Jia, W., and Zhang, J. (2008). AtMKK1 mediates ABA-*induced CAT1* expression and H_2O_2 production via AtMPK6-coupled signaling in Arabidopsis. Plant J. **54:** 440–451.

Xiong, L., Schumaker, K.S., and Zhu, J.-K. (2002). Cell signaling during cold, drought, and salt stress. Plant Cell **14** (suppl.)**:** S165–S183.

Xu, J., Li, H.-D., Chen, L.-Q., Wang, Y., Liu, L.-L., He, L., and Wu, W.-H. (2006). A protein kinase, interacting with two calcineurin B-like proteins, regulates K^+ transporter AKT1 in *Arabidopsis.* Cell **125:** 1347–1360.

Xu, J., Tian, Y.-S., Peng, R.-H., Xiong, A.-S., Zhu, B., Jin, X.-F., Gao, F., Fu, X.-Y., Hou, X.-L., and Yao, Q.-H. (2010). AtCPK6, a functionally redundant and positive regulator involved in salt/drought stress tolerance in Arabidopsis. Planta **231:** 1251–1260.

Yang, T., and Poovaiah, B.W. (2002). Hydrogen peroxide homeostasis: activation of plant catalase by calcium/calmodulin. Proc. Natl. Acad. Sci. USA **99:** 4097–4102.

Zhang, X., Zhang, L., Dong, F., Gao, J., Galbraith, D.W., and Song, C.-P. (2001a). Hydrogen peroxide is involved in abscisic acid-induced stomatal closure in *Vicia faba.* Plant Physiol. **126:** 1438–1448.

Zhang, X., Miao, Y.C., An, G.Y., Zhou, Y., Shangguan, Z.P., Gao, J.F., and Song, C.P. (2001b). K^+ channels inhibited by hydrogen peroxide mediate abscisic acid signaling in *Vicia* guard cells. Cell Res. **11:** 195–202.

Zhao, L.-N., Shen, L.-K., Zhang, W.-Z., Zhang, W., Wang, Y., and Wu, W.-H. (2013). Ca^{2+}-dependent protein kinase11 and 24 modulate the activity of the inward rectifying K^+ channels in Arabidopsis pollen tubes. Plant Cell **25:** 649–661.

Zhao, R., Sun, H.-L., Mei, C., Wang, X.-J., Yan, L., Liu, R., Zhang, X.-F., Wang, X.-F., and Zhang, D.-P. (2011). The Arabidopsis Ca^{2+}-dependent protein kinase CPK12 negatively regulates abscisic acid signaling in seed germination and post-germination growth. New Phytol. **192:** 61–73.

Zhou, H., Zhao, J., Yang, Y., Chen, C., Liu, Y., Jin, X., Chen, L., Li, X., Deng, X.W., Schumaker, K.S., and Guo, Y. (2012). Ubiquitin-specific protease16 modulates salt tolerance in *Arabidopsis* by regulating Na^+/H^+ antiport activity and serine hydroxymethyltransferase stability. Plant Cell **24:** 5106–5122.

Zhou, L., Lan, W., Jiang, Y., Fang, W., and Luan, S. (2014). A calcium-dependent protein kinase interacts with and activates a calcium channel to regulate pollen tube growth. Mol. Plant **7:** 369–376.

Zhu, S.-Y., et al. (2007). Two calcium-dependent protein kinases, CPK4 and CPK11, regulate abscisic acid signal transduction in *Arabidopsis.* Plant Cell **19:** 3019–3036.

Zielinski, R.E. (1998). Calmodulin and calmodulin-binding proteins in plants. Annu. Rev. Plant Physiol. Plant Mol. Biol. **49:** 697–725.

Zimmermann, P., Heinlein, C., Orendi, G., and Zentgraf, U. (2006). Senescence-specific regulation of catalases in *Arabidopsis thaliana* (L.) Heynh. Plant Cell Environ. **29:** 1049–1060.

Zou, J.-J., Wei, F.-J., Wang, C., Wu, J.-J., Ratnasekera, D., Liu, W.-X., and Wu, W.-H. (2010). Arabidopsis calcium-dependent protein kinase CPK10 functions in abscisic acid- and Ca^{2+}-mediated stomatal regulation in response to drought stress. Plant Physiol. **154:** 1232–1243.

Arabidopsis CALCIUM-DEPENDENT PROTEIN KINASE8 and CATALASE3 Function in Abscisic Acid-Mediated Signaling and H_2O_2 Homeostasis in Stomatal Guard Cells under Drought Stress

Jun-Jie Zou, Xi-Dong Li, Disna Ratnasekera, Cun Wang, Wen-Xin Liu, Lian-Fen Song, Wen-Zheng Zhang and Wei-Hua Wu

Plant Cell; originally published online May 12, 2015;
DOI 10.1105/tpc.15.00144